JOURNAL OF BACTERIOLOGY, June 2010, p. 3187–3203 Vol. 192, No. 12
0021-9193/10/$12.00 doi:10.1128/JB.01558-09

Role of the FeoB Protein and Siderophore in Promoting Virulence of *Xanthomonas oryzae* pv. oryzae on Rice[▽]

Alok Pandey and Ramesh V. Sonti*

Centre for Cellular and Molecular Biology, Council of Scientific and Industrial Research, Uppal Road, Hyderabad 500 007, Andhra Pradesh, India

Received 30 November 2009/Accepted 22 March 2010

***Xanthomonas oryzae* pv. oryzae causes bacterial blight, a serious disease of rice. Our analysis revealed that the *X. oryzae* pv. oryzae genome encodes genes responsible for iron uptake through FeoB (homolog of the major bacterial ferrous iron transporter) and a siderophore. A mutation in the *X. oryzae* pv. oryzae *feoB* gene causes severe virulence deficiency, growth deficiency in iron-limiting medium, and constitutive production of a siderophore. We identified an iron regulated *xss* gene cluster, in which *xssABCDE* (*Xanthomonas* siderophore synthesis) and *xsuA* (*Xanthomonas* siderophore utilization) genes encode proteins involved in biosynthesis and utilization of *X. oryzae* pv. oryzae siderophore. Mutations in the *xssA*, *xssB*, and *xssE* genes cause siderophore deficiency and growth restriction under iron-limiting conditions but are virulence proficient. An *xsuA* mutant displayed impairment in utilization of native siderophore, suggesting that XsuA acts as a specific receptor for a ferric-siderophore complex. Histochemical and fluorimetric assays with *gusA* fusions indicate that, during *in planta* growth, the *feoB* gene is expressed and that the *xss* operon is not expressed. This study represents the first report describing a role for *feoB* in virulence of any plant-pathogenic bacterium and the first functional characterization of a siderophore-biosynthetic gene cluster in any xanthomonad.**

Iron is one of the most important nutrients for bacterial growth. Although iron is abundant in nature, its availability is limiting because of low solubility (9). Bacteria encode multiple iron uptake pathways, which provide specificities and affinities for various forms of environmental or host iron. Under iron-limited conditions bacteria secrete siderophores (low-molecular-weight iron chelators), which facilitate ferric iron acquisition. This ferric-siderophore complex is taken up into bacterial cells by a transporter system comprised of a TonB-ExbBD-dependent outer membrane receptor, a periplasmic binding protein, and an inner membrane ABC permease complex (33, 46). Siderophores can be classified into three major classes based on the ligand that participates in chelating iron and are either catecholates (e.g., enterobactin), hydroxamates (e.g., alcaligin), or α-hydroxy carboxylates (e.g., vibrioferrin). Some siderophores belong to a class of mixed-type siderophores (e.g., aerobactin) (43). A number of siderophores are synthesized as small peptides by multimodular enzymes known as nonribosomal peptide synthetases (NRPSs) (17) while other siderophores are nonpolypeptidic in nature and are synthesized via NRPS-independent pathways (13).

Extensive studies have shown the importance of siderophores in virulence of a number of animal-pathogenic bacteria. For instance, the siderophore pyoverdine is essential for virulence of *Pseudomonas aeruginosa*, and production of yersiniabactin is required for full virulence of *Yersinia pestis* and *Klebsiella pneumoniae* (3, 34, 42). The plant-pathogenic bacterium *Erwinia chrysanthemi* strain 3937, which causes soft rot disease on a variety of plants, produces two siderophores, namely, achromobactin and chrysobactin, both of which are required for optimal virulence on African violets (*Saintpaulia ionantha*) (23). Siderophore-deficient mutants of *Erwinia amylovora* are virulence deficient on apple (22). However, *Pseudomonas syringae* pv. syringae B301D, a pathogen of stone fruit trees, does not require pyoverdine for virulence (16). *P. syringae* pv. tomato DC3000, the causal agent of bacterial speck disease of tomato, produces yersiniabactin as well as pyoverdine. Yersiniabactin is produced *in planta*, and the *pchA* gene encoding isochorismate synthase is required to synthesize it. However, a *pchA* mutant of this bacterium does not show any growth defect or altered virulence on tomato and *Arabidopsis* hosts (30). Also, siderophore-deficient mutants of the plant pathogens *Ralstonia solanacearum*, *Erwinia carotovora* subsp. *carotovora*, and *Agrobacterium tumefaciens* retain virulence proficiency (5, 11, 38, 58). These findings suggest that there is considerable variation in the contributions of siderophores to plant-bacteria interactions.

In addition to the uptake of ferric iron, many bacteria take up free ferrous iron via the Feo (ferrous iron transporter) system (12). The Feo system encoded by the *feoABC* operon is well characterized in *Escherichia coli*. The *feoB* gene encodes the major bacterial ferrous iron transporter composed of a hydrophilic cytoplasmic domain and an integral membrane domain (31). The cytoplasmic domain of the FeoB protein in *E. coli* has been shown to act as a GTPase and exhibits sequence similarities to eukaryotic G proteins (40). Binding of GTP/GDP is required for efficient uptake of ferrous iron through the FeoB-dependent transport system. The roles of *feoA* and *feoC* are not known, but they are predicted to encode a GTPase-activating protein (GAP) and an Fe-S cluster containing a transcriptional regulator, respectively (12). In animal-pathogenic bacteria such as *E. coli*, *Helicobacter pylori*, *Legionella pneumophila*, *Salmonella enterica* serovar Typhimurium,

* Corresponding author. Mailing address: Centre for Cellular and Molecular Biology, Uppal Road, Hyderabad 500007, Andhra Pradesh, India. Phone: 91 40 27192577. Fax: 91 40 27160591. E-mail: sonti@ccmb.res.in.

▽ Published ahead of print on 9 April 2010.

Porphyromonas gingivalis, and *Campylobacter jejuni*, mutation in the *feoB* gene has been shown to cause deficiency in ferrous iron uptake and virulence (8, 19, 45, 57, 65, 71). There is no report on the role of *feoB* in virulence of any plant-pathogenic bacterium.

Although iron is essential for bacterial growth, excess intracellular iron is toxic because of the generation of free radicals (70). Hence, the expression of iron acquisition functions must be tightly controlled, and this function is performed by the ferric uptake regulator (Fur) protein. By using ferrous ion as a corepressor, Fur functions as a transcriptional repressor of iron uptake-related genes in bacteria. Fur binds to specific sequences called Fur boxes that are located in the promoter regions of such genes (51).

The Gram-negative bacterial genus *Xanthomonas* comprises bacteria that cause almost ~400 different plant diseases (14). In *Xanthomonas campestris* pv. campestris, which causes black rot of cruciferous plants, a *tonB* mutant is impaired for ferric ion uptake and exhibits increased extracellular siderophore production and reduced disease symptoms (72, 73). In *Xanthomonas oryzae* pv. oryzae, causal agent of the serious bacterial blight disease of rice, a *fur* mutant exhibits a severe *in planta* growth deficiency that appears to be due to increased oxidative stress (66). In *X. campestris* pv. phaseoli, which causes common bacterial blight of beans, the Fur protein has been characterized with respect to primary structure (39).

X. oryzae pv. oryzae uses a diverse array of functions to grow within the xylem vessels of rice leaves and cause disease (47). In this study, we have assessed the role of two different iron uptake systems in promoting virulence of *X. oryzae* pv. oryzae. We have mutated the *feoB* homolog of this bacterium and demonstrated that this results in a severe virulence deficiency. We have also determined that the *xss* operon of *X. oryzae* pv. oryzae is involved in siderophore biosynthesis and transport. Mutations in the *xss* operon result in siderophore deficiency but do not affect virulence.

MATERIALS AND METHODS

Bacterial strains, plasmids, primers, and culture media. Bacterial strains and plasmids used in this study are listed in Table 1. Primers and degenerate primers used in this work are listed in Table 2 and Table 3, respectively. Degenerate primers were designed based on sequences of *X. campestris* pv. campestris strain ATCC 33913 and *Xanthomonas axonopodis* pv. citri strain 306 using the CODEHOP (consensus-degenerate hybrid oligonucleotide primers) program (59). *X. oryzae* pv. oryzae strains were grown at 28°C in peptone sucrose (PS) medium, and *E. coli* strains were grown at 37°C in Luria Bertani (LB) medium as described previously (55). To minimize contamination with exogenous iron, MilliQ water and acid-washed glassware were used in this study. The concentrations of antibiotics used in this study were as follows: rifampin (Rf), 50 μg/ml; ampicillin (Ap), 100 μg/ml; spectinomycin (Sp), 50 μg/ml; kanamycin (Km), 50 μg/ml for *E. coli* and 15 μg/ml for *X. oryzae* pv. oryzae; and tetracycline (Tc). 15 μg/ml for *E. coli* and 5 μg/ml for *X. oryzae* pv. oryzae.

Molecular biological and microbiological techniques. Genomic DNA isolation was performed as described by Leach et al. (35). Plasmid DNA was isolated by the alkaline lysis method (61) or by using a Qiagen plasmid midi-kit. Phusion polymerase (Finnzymes) was used for PCR amplification in applications that required high-fidelity DNA synthesis (such as for complementation analysis) while *Taq* polymerase was used for all other applications. Restriction digestions were done with enzymes from New England Biolabs (NEB; Beverly, MA). PCR products and restriction enzyme-digested DNA fragments were purified using a QIAquick PCR purification kit and a QIAquick nucleotide removal kit (Qiagen), respectively. Other techniques such as ligation with T4 DNA ligase, agarose gel electrophoresis, and transformation of *E. coli* were performed as described previously (61). Plasmids were transferred from *E. coli* to *X. oryzae* pv. oryzae using either broad-host-range mobilizing strain S17-1 (64) for biparental matings or electroporation (55, 66).

DNA sequencing and bioinformatics tools. Sequencing was performed with an ABI Prism 3700 automated DNA sequencer (Perkin-Elmer, Foster City, CA). Homology and conserved domain searches were performed in the NCBI database by using the BLAST algorithm (2). Pairwise alignment was carried out using Clustal W (69). The presence of transmembrane helices in proteins was predicted using TMpred and TMHMM, version 2.0, programs at the ExPASy proteomics server. The PSORTb program was used for the prediction of subcellular localization of bacterial proteins (26).

RNA isolation, operon mapping, and expression analysis. To investigate the transcriptional organization and expression of *feoABC* genes and the *xss* gene cluster, reverse transcription-PCR (RT-PCR) was performed with total RNA isolated from *X. oryzae* pv. oryzae strain BXO43 grown under iron-supplemented and iron-limiting conditions. A culture of *X. oryzae* pv. oryzae grown in PS medium to an optical density at 600 nm (OD_{600}) of 0.5 was split into two parts. Ferrous sulfate ($FeSO_4$) was added at 100 μM to one part (iron-supplemented conditions), and 2,2′-dipyridyl (DP; an iron chelator) was added at 100 μM to the other part (iron-limiting conditions). Both cultures were further incubated for 6 h, and total RNA from each of the samples was isolated using TRIzol reagent (Invitrogen). Total RNA concentration was determined spectrophotometrically. RNA samples were treated with RNase-free DNase I (Promega) for 1 h at 37°C to remove any DNA contamination. A total of 5 μg of RNA was reverse transcribed using SuperscriptIII RT enzyme (Invitrogen) as per the supplier's instructions. For *feo* operon mapping, cDNA synthesis was performed with primer FeoCR, complementary to the *feoC* gene. The resulting cDNAs were used as a template for PCR amplification with *Taq* polymerase using specific primer pairs for each gene. The following primer pairs were used: FeoCR/FeoBF2 for amplification of *feoCB* and FeoBR1/FeoAF for the *feoBA* region. To detect the presence or absence of *feoB* transcripts, PCR was done with FeoBF and FeoBR primers. To determine the transcriptional organization and iron-mediated regulation of the *xss* gene cluster, cDNA synthesis was done using RNA isolated from iron-supplemented and iron-limiting conditions, with primer MF1 which is complementary to the *xssE* gene. Subsequent PCR was done with cDNA as a template. To amplify the *xssE-xssD*, *xssB-xssA*, and *xsuA-mhpE* regions, MF1/MR2, MF3/MR4, and MF5/MR6 primer pairs were used, respectively. RT-PCR products were analyzed on a 1.2% agarose gel along with a 100-bp DNA ladder (NEB). Sequencing of RT-PCR-amplified products was done to confirm their identity.

Construction of *feo*::*gusA* and *xssE*::*gusA* strains. Glucuronidase (GUS) reporter gene fusions were created by using the suicide plasmid pVO155 that has the promoterless *gusA* gene (48). To construct the *feo*::*gusA* transcriptional fusion, a 343-bp DNA fragment containing the putative promoter of the *feoABC* operon (+139 to −224) was amplified by using the FBPFB/FBPFX primers. This promoter fragment was subsequently digested with BamHI and XbaI and directionally cloned upstream of the promoterless *gusA* gene in to similarly digested pVO155 to create the *feo*::*gusA* reporter construct pAP17. To create an *xssE*::*gusA* fusion, a 503-bp PCR-amplified internal fragment of the *xssE* gene was cloned into the pCR-Blunt-II-TOPO vector to obtain the plasmid pAP4. This plasmid was digested with SpeI and XbaI, and the released fragment was directionally cloned upstream of the promoterless *gusA* gene into the similarly digested pVO155 to create the *xssE*::*gusA* reporter construct, pAP16. After confirmation by sequencing, the resulting pAP17 and pAP16 constructs were then introduced in to strain BXO43 by biparental mating using *E. coli* S17-1. *X. oryzae* pv. oryzae GUS reporter strains were selected on medium plates containing rifampin (counter-selectable marker) and kanamycin. Since pVO155 cannot replicate in *X. oryzae* pv. oryzae, kanamycin-resistant colonies are obtained upon chromosomal integration of the plasmid using the cloned DNA sequence as a region of homology. Chromosomal integration of the plasmid was confirmed by PCR using flanking primers (from the chromosomal region of interest) and the vector-specific primers PVO155F/PVO155R and sequencing of the PCR product. The *feo*::*gusA* and *xssE*::*gusA* transconjugants were named BXO2230 and BXO2229, respectively. In BXO2230, P_{feoABC} is fused to *gusA* and leaves an intact functional *feoABC* operon with its associated native promoter. In BXO2229, the *gusA* fusion leads to disruption of *xssE*.

β-Glucuronidase reporter assays. GUS reporter strains were grown to an OD_{600} of 0.6 in PS medium. Aliquots of 1.1 ml of the cell suspension were taken, and either $FeSO_4$ (at a final concentration of 25 μM or 100 μM to obtain iron supplementation) or DP (at a final concentration of 25 μM, 50 μM, or 100 μM to cause iron limitation) was added. In addition to the above, several 1.1-ml aliquots of the strains were grown without any supplementation. All of these cultures were incubated at 28°C for a further period of 6 h, and 100 μl was

TABLE 1. Bacterial strains and plasmids used in this study

Strain or plasmid	Relevant characteristic(s)[a]	Reference or source
E. coli strains		
DH5α	λ$^-$ f80d*lacZ*DM15 D(*lacZYA-argF*)*U169 recA1 endA hsdR17*(r_K^- m_K^-) *supE44 thi-1 gyrA relA1*	Invitrogen
S17-1	RP4-2 Tc::Mu-Km::Tn*7 pro hsdR recA* Tra$^+$; used as a mobilizing strain	64
X. oryzae pv. oryzae strains		
BXO1	Wild type; Indian isolate	Lab collection
BXO43	*rif-2*; derivative of BXO1	Lab collection
BXO2201	*feoB1*::pK18*mob rif-2*; Km^r; derived from BXO43	This work
BXO2204	*feoB1*::pK18*mob rif-2*/pHM1; Km^r Sp^r	This work
BXO2206	*feoB1*::pK18*mob rif-2*/pAP3 *feoB*$^+$; Km^r Sp^r	This work
BXO2211	*xssE1*::pK18*mob rif-2*; Sid$^-$ Km^r; derived from BXO43	This work
BXO2214	*xssB1*::pK18*mob rif-2*; Sid$^-$ Km^r; derived from BXO43	This work
BXO2217	*xssA1*::pK18*mob rif-2*; Sid$^-$ Km^r; derived from BXO43	This work
BXO2220	*mhpE1*::pK18*mob rif-2*; Sid$^+$ Km^r; derived from BXO43	This work
BXO2223	*xssE1*::pK18*mob rif-2*/pAP15; Sid$^+$ Km^r Tc^r	This work
BXO2224	*xssB1*::pK18*mob rif-2*/pAP15; Sid$^+$ Km^r Tc^r	This work
BXO2225	*xssA1*::pK18*mob rif-2*/pAP15; Sid$^+$ Km^r Tc^r	This work
BXO2229	*xssE2*::*gusA rif-2*; Sid$^-$ Km^r; derived from BXO43	This work
BXO2230	*feo*::*gusA rif-2*; Km^r *feoB*$^+$; derived from BXO43	This work
BXO2231	*xsuA1*::*gusA rif-2*; Km^r; derived from BXO43	This work
BXO2233	*xsuA1*::*gusA rif-2*/pAP23; Km^r Tc^r	This work
BXO2234	*xsuA1*::*gusA rif-2*/pAP15; Km^r Tc^r	This work
BXO2235	*xsuA2*::pK18*mob rif-2*; Km^r; derived from BXO43[c]	This work
BXO2236	*xsuA3*::pK18*mob rif-2*; Km^r; derived from BXO43[b]	This work
Plasmids		
pCR-Blunt II-TOPO	PCR cloning vector; Km^r	Invitrogen
pMOS*blue*	High-copy-number cloning vector; Ap^r	Amersham Pharmacia Biotech
pK18*mob*	pUC18 derivative; Mob$^+$ Km^r; does not replicate in *X. oryzae* pv. oryzae	62
pHM1	Broad-host-range cosmid vector (~13.3 kb); Sp^r	28
pBSKS+	*E. coli* cloning vector; Ap^r	Stratagene
pUFR034	*IncW*; Km^r Mob$^+$ *mob* (P) *lacZ*α$^+$ Par$^+$ *cos* (8.7 kb)	21
pTc28	Source of tetracycline cassette; Tc^r Ap^r	56
pVO155	pUC119 derivative carrying promoterless *gusA*; Km^r Ap^r	48
pAP1	pCR-Blunt II-TOPO with 510-bp internal fragment of *feoB*	This work
pAP2	pK18*mob* with 510-bp fragment of *feoB* (from pAP1) cloned in to EcoRI site of pK18*mob*	This work
pAP3	pHM1 with 2,119-bp fragment containing full length *feoB* cloned in to HindIII and SacI sites of pHM1	This work
pAP4	pCR-Blunt II-TOPO with 503-bp internal fragment of *xssE*	This work
pAP5	pK18*mob* with 503-bp fragment of *xssE* (from pAP4) cloned in to EcoRI site of pK18*mob*	This work
pAP6	pMOS*blue* with 553-bp internal fragment of *xssB*	This work
pAP7	pK18*mob* with 553-bp fragment of *xssB* (from pAP6) cloned in to EcoRI and HindIII sites of pK18*mob*	This work
pAP8	pCR-Blunt II-TOPO with 512-bp internal fragment of *xssA*	This work
pAP9	pK18*mob* with 512-bp fragment of *xssA* (from pAP8) cloned in to PstI and HindIII sites of pK18*mob*	This work
pAP10	pMOS*blue* with 339-bp internal fragment of *mhpE*	This work
pAP11	pK18*mob* with 339-bp fragment of *mhpE* (from pAP10) cloned in to EcoRI and HindIII sites of pK18*mob*	This work
pAP12	pUFR034 with 38.2-kb genomic insert of *X. oryzae* pv. oryzae containing entire *xss* gene cluster	This work
pAP13	~2.4kb *tet* cassette from pTc28 cloned in to the XbaI and KpnI sites of pMOS*blue*; Tc^r Ap^r	This work
pAP14	pBSKS with 2.4-kb *tet* cassette (from pAP13) cloned in to XbaI and SacI sites of pBSKS; Tc^r Ap^r	This work
pAP15	Tc^r Km^s; derivative of pAP12 (*tet* cassette from pAP14 cloned in to XhoI site of pAP12)	This work
pAP16	pVO155 with 503-bp fragment of *xssE* (from pAP4) cloned in to SpeI and XbaI sites of pVO155	This work
pAP17	pVO155 carrying 343-bp DNA (putative promoter region, +139 to −114) upstream of *feoABC* operon	This work
pAP18	pCR-Blunt II-TOPO with 505-bp internal fragment of *xsuA*	This work
pAP19	pVO155 with 505-bp fragment of *xsuA* (from pAP18) cloned in to SpeI and XhoI sites of pVO155	This work
pAP20	pK18*mob* with 505-bp fragment of *xsuA* (from pAP18) cloned in to EcoRI site of pK18*mob*; nonpolar version (*lacZ* promoter of pK18*mob* and *xsuA* gene fragment are in the same transcriptional orientation)	This work
pAP21	pK18*mob* with 505-bp fragment of *xsuA* (from pAP18) cloned in to EcoRI site of pK18*mob*; polar version (*lacZ* promoter of pK18*mob* and *xsuA* gene fragment are in opposite transcriptional orientations)	This work
pAP22	A 9.9-kb DNA fragment containing *xsuA* gene from pAP12 cloned into EcoRI site of pUFR034	This work
pAP23	Tc^r Km^s; derivative of pAP22 (*tet* cassette from pAP14 cloned into XhoI site of pAP22)	This work

[a] The *rif-2* mutation confers resistance to rifampin; Ap^r, Sp^r, Tc^r, and Km^r indicate resistance to ampicillin, spectinomycin, tetracycline, and kanamycin, respectively. Km^s indicates kanamycin sensitivity. Sid$^+$ and Sid$^-$ indicate proficiency and deficiency in siderophore production, respectively.
[b] Polar mutation in *xsuA*.
[c] Nonpolar mutation in *xsuA*.

removed to determine the number of CFU/ml. The remaining 1 ml of culture was centrifuged, and the obtained pellet was then washed once in sterile MilliQ water to remove the residual supplements. The cell pellets were resuspended in 250 μl of 1 mM MUG (4-methylumbelliferyl β-D-glucuronide) extraction buffer (50 mM sodium dihydrogen phosphate [pH 7.0], 10 mM EDTA, 0.1% Triton X-100, 0.1% sodium lauryl sarcosine, and 10 mM β-mercaptoethanol) (29) and incubated at 37°C. Subsequently, 25-μl aliquots were taken from each reaction mixture, and the reaction was terminated at suitable time intervals by the addition of 225 μl of 0.2 M Na_2CO_3. Fluorescence was measured on a Spectramax Gemini XS dual scanning microplate spectrofluorimeter (Molecular Devices) with 4-methyl-umbelliferone (MU; Sigma) as the standard. β-Glucuronidase activity was expressed as nanomoles of MU produced/minute/10^8 CFU.

Generation and complementation of the *X. oryzae* pv. oryzae *feoB* mutant. The *X. oryzae* pv. oryzae *feoB* gene was disrupted by homologous suicide plasmid integration using vector pK18*mob* (62). A 510-bp internal fragment of the *feoB* gene was amplified by PCR using genomic DNA of *X. oryzae* pv. oryzae strain BXO43 and the gene-specific FeoBF/FeoBR primer pair and cloned into pCR-Blunt II-TOPO vector (Invitrogen) to generate the plasmid pAP1. The cloned DNA fragment was excised from pAP1 using EcoRI and further cloned into EcoRI-digested pK18*mob* to create the plasmid pAP2. This construct was then

TABLE 2. Oligonucleotide primers used in this study

Primer name	Nucleotide sequence (5′–3′ [restriction site])[a]
M13F	GTAAAACGACGGCCAGT
M13R	GGAAACAGCTATGACCATG
T7	TAATACGACTCACTATAGGG
FeoBF	CGGTGGTGATGTTCCTGATCTT
FeoBR	ACAGCACCAATCCCTGCTGATT
FeoBFF	GACGTGCTGGTCTACGTGA
FeoBRR	CGGCCTGCGAAGCTGTAGT
FeoAHF	CCCAAGCTTGGGGAGGAAGTCACGGTGC TGGC (HindIII)
FeoCSR	CGAGCTCGGACCACGTGCAAGCGCACGA (SacI)
1354F	CAAACTCGATACCGAGCTCGC
1354R	GCAGGTCTGTGCCATGTTCG
1354FF	GCGCATACGTCTACGACCT
1354RR	TGCCAGCACATCCTTGGGT
1357F	CCGGCAGAGTTATGGCCGAGT
1357R	ACCAGTGCAGCACATCGCCGT
1357FF	AACATGGTACGCACGCATGGT
1357RR	GCGCGGGCTGCCATTCGGTAA
1358F	CTATGCCGCCAAGAACAAGGC
1358R	CGATGCTGCGGTAATTGATCT
1358FF	ATCACCTGGCCTATTTCCACG
1358RR	CACGCCCAGGTAATCCTTGTT
1359F	AGCGTTATCTGGTCGACAT
1359R	GTAATGGCGTTGCTGACGTA
1359FF	AGATCGACCGCATCGACAT
1359RR	TGTTATCCAGTTGGATCTGCT
1360F	CGATGAACTTGAACATGCCATC
1360R	ACGGCGAGAATTTCCGGAAG
1360FF	CTCAATGCAGTGCCAAGCGT
1360RR	CAATGCGCGTTGAATCAGTG
MF1	GCTGCCTGGGCGAGCTCGGTATC
MR2	CTGCAGAACACGGTGATCGGTTTC
MF3	CACTCATGCGTTGCAACCATGC
MR4	CGGTGCTTGTGGAGATCAATTAC
MF5	CGGTTTCGTCGAAGATCTTGAT
MR6	CATCGTGCCGATGATCGAAAG
FBPFB	CGGGATCCCGCGATCAGTGTCGCATC GAAG (BamHI)
FBPFX	GCTCTAGAGCCACCGTGACTTCCTCG CCAG (XbaI)
PVO155F	CCGCCTAATGAGCGGGCTT
PVO155R	GATCCAGACTGAATGCCCACA
FeoAF	GAGGAAGTCACGGTGCTGGC
FeoCR	GACCACGTGCAAGCGCACGA
FeoBF2	GGACGATGAAGAAGTGGCG
FeoBR1	CCAGATCGGATGCAGCAAC

[a] The engineered restriction modification sites are underlined. All of the primers were developed in the course of this study.

TABLE 3. List of degenerate oligonucleotide primers used in this study

Primer name	Target gene[a]	Nucleotide sequence (5′–3′)[b]
AP2F	*xssA*	CCTGCCGGGCAAG**GAYTGGCARGT**
AP2R		GGCGTCCCACTGG**GCYTCRCAYTC**
AP3F	*xssB*	CCACTACGCCCCG**GARTTYGCNCC**
AP3R		AAGCTCTCGGCCAGG**GDATNGCCAT**
AP4F	*xssD*	GCGTGCGCAAGAAC**GCNTGGTAYGA**
AP4R		CGCGGGTC**GGCCANCCRTC**
AP5F	*xssE*	GGTGTTCCTGCG**CATGAAYATHGC**
AP5R		CGCGGCACGGG**TGRTCRTGNCC**
AP6F	*xsuA*	GCGCGTGCGC**GCNGARTGGTG**
AP6R		CGCCGGCG**GTCCAYTGYTG**
AP7F	*xssC*	CCCGCGCCCTG**GAYTGGACNCA**
AP7R		CGTCGCCGCGG**CKCCACCANGG**

[a] Intragenic fragments were amplified from BXO43 genomic DNA.

[b] The region of degeneracy is indicated by boldface letters. In the sequences, Y is C or T; R is A or G; K is G or T; D is A, G, or T; H is A, C, or T; and N is A, C, G, or T. All of the primers were developed in the course of this study.

transferred from *E. coli* strain S17-1 to *X. oryzae* pv. oryzae via biparental mating, and *feoB* gene disruptants were selected on kanamycin-containing medium. Gene disruption was confirmed by PCR using flanking gene-specific primers FeoBFF/FeoBRR (which bind in chromosomal regions that flank the insert sequence cloned in pAP2) in combination with vector-specific primers M13F and M13R and sequencing of the PCR products. In pAP2, the transcriptional orientations of the *lacZ* promoter of pK18*mob* and of the *feoB* gene fragment were in the same direction so that mutation caused by pAP2 integration is unlikely to cause any polar effect on downstream genes due to activity of the *lacZ* promoter (74). One of the confirmed mutants was named BXO2201 and was chosen for further study. For *feoB* mutant complementation, a 2,119-bp DNA fragment containing the entire *feoB* coding region with its own ribosomal binding site and extending from 125 bp upstream of the start codon to 128 bp downstream of the stop codon of the *feoB* gene was amplified by PCR using the total DNA of *X. oryzae* pv. oryzae and primers FeoAHF/FeoCSR. The amplified fragment was cloned as an HindIII-SacI fragment into broad-host-range vector pHM1 (28) to create recombinant plasmid pAP3. The pAP3 clone and pHM1 vector were individually introduced in to the *feoB* mutant strain (BXO2201) to obtain strains BXO2206 (*feoB*/pAP3; for complementation) and BXO2204 (*feoB*/pHM1; control).

Isolation of a cosmid clone containing the entire *xss* gene cluster from a *X. oryzae* pv. oryzae genomic library. A genomic library of *X. oryzae* pv. oryzae (average insert size of 30 kb) had been constructed in the cosmid vector pUFR034 (21) and maintained in *E. coli* strain S17-1 (54). A total of 480 clones were screened by PCR using 1354F/1354R (*xssE*-specific), 1358F/1358R (*xssA*-specific) and 1360F/1360R (*mhpE*-specific) primer pairs. Five positive clones were identified, and one of these clones (named pAP12) with an insert size of ~38.2 kb was characterized further. End sequencing of this clone was performed with M13F and M13R primers, which indicated that the cloned DNA extends from the XOO1344 gene to the XOO1371 gene (as per nomenclature for *X. oryzae* pv. oryzae strain KACC10331 [36]) while the entire *xss* gene cluster ranges from XOO1354 to XOO1360.

Construction and complementation analyses of *xssA*, *xssB*, *xssE*, *mhpE*, and *xsuA* mutants. The *xssA*, *xssB*, *xssE*, and *mhpE* genes were each disrupted by integration of suicide plasmid pK18*mob*. Three different *xsuA* mutants were created by integration of either pK18*mob* or pVO155 (Table 4 lists the primers and plasmids used, steps for mutant construction, and the designation for each mutant).

A kanamycin resistance determinant is present in the *xss* mutants (BXO2211, BXO2214, and BXO2217) as well as in the pAP12 cosmid. Therefore, the kanamycin resistance gene of pAP12 was inactivated by insertion of a tetracycline (*tet*) resistance cassette. To do so, a 2.4-kb *tet* cassette was excised from the pTc28 vector (56) using XbaI and KpnI and subsequently cloned into the XbaI and KpnI site of pMOS*Blue* to obtain pAP13. The *tet* cassette was released from pAP13 by double digestion with XbaI and SacI and then cloned into similarly digested the pBSKS+ (Stratagene) plasmid to obtain pAP14. Subsequently, pAP14 was digested with XhoI to release the *tet* cassette, which was ligated to XhoI-digested pAP12 to generate pAP15, which was electroporated into BXO2211, BXO2214, and BXO2217 (by selection for tetracycline resistance) to generate complemented strains BXO2223, BXO2224, and BXO2225, respectively. For genetic complementation of BXO2231 (*xsuA* mutant), a 9.9-kb EcoRI fragment, which includes the full-length *mhpE* and *xsuA* genes but not the *xss* gene, was obtained after digestion of the cosmid pAP12 with EcoRI. This 9.9-kb DNA fragment was cloned into EcoRI-digested pUFR034 to obtain the cosmid pAP22. The kanamycin resistance marker of cosmid pAP22 was then inactivated by insertion of the *tet* cassette. This was accomplished by digesting pAP14 with XhoI to release the *tet* cassette, which was ligated to XhoI-digested pAP22 to generate the cosmid pAP23. Cosmids pAP23 and pAP15 were electroporated into BXO2231 by selection for tetracycline resistance to generate complemented strains BXO2233 and BXO2234, respectively.

Siderophore production assay. Peptone-sucrose agar (PSA)-chrome azurol sulfonate (CAS) siderophore indicator plates (63) were prepared as described previously (15). In order to create iron-limiting conditions, DP (100 μM) was added to PSA-CAS plates. The colonies were then scored for the orange halo phenotype that is indicative of siderophore production. Csaky and Arnow tests (52) were used to test for production of hydroxamate and catechol-type siderophores, respectively. Deferoxamine mesylate ([DFX] a trihydroxamate sid-

TABLE 4. Construction of *X. oryzae* pv. oryzae *xssE*, *xssB*, *xssA*, *mhpE*, and *xsuA* mutants

Gene	Primer pair for amplification (length of internal gene fragment [bp])	Plasmid clone (cloning vector)	Restriction enzyme(s)	Plasmid clone used for gene disruption (suicide vector)[a]	Mutant strain	Primer pair used to confirm gene disruption	
						Gene specific	Vector specific
xssE	1354F/1354R (503)	pAP4 (pCR-Blunt-II-TOPO)	EcoRI	pAP5 (pK18*mob*)[b]	BXO2211	1354FF/1354RR	M13F/M13R
xssB	1357F/1357R (553)	pAP6 (pMOS*blue*)	EcoRI-HindIII	pAP7 (pK18*mob*)[b]	BXO2214	1357FF/1357RR	M13F/M13R
xssA	1358F/1358R (512)	pAP8 (pCR-Blunt-II-TOPO)	PstI-HindIII	pAP9 (pK18*mob*)[b]	BXO2217	1358FF/1358RR	M13F/M13R
mhpE	1360F/1360R (339)	pAP10 (pMOS*blue*)	EcoRI-HindIII	pAP11 (pK18*mob*)[b]	BXO2220	1360FF/1360RR	M13F/M13R
xsuA	1359F/1359R (505)	pAP18 (pCR-Blunt-II-TOPO)	SpeI-XhoI	pAP19 (pVO155)	BXO2231	1359FF/1359RR	PVO155F/PVO155R
			EcoRI	pAP20 (pK18*mob*)[b]	BXO2235	1359FF/1359RR	M13F/M13R
			EcoRI	pAP21 (pK18*mob*)[c]	BXO2236		

[a] These constructs were transferred from *E. coli* strain S17-1 to *X. oryzae* pv. oryzae via biparental matings, and gene disruptants were selected on kanamycin-containing medium.

[b] The transcriptional orientation of the *lacZ* promoter of pK18*mob* is in the same direction as the cloned gene fragment. Therefore, integration of the plasmid is likely to result in a nonpolar mutation.

[c] The transcriptional orientation of the *lacZ* promoter of pK18*mob* is in the opposite direction of the cloned gene fragment. Therefore, plasmid integration will result in a polar mutation.

erophore; Sigma) and 2,3-dihydroxy benzoic acid ([DHBA] a catechol siderophore; Sigma) were used as positive controls.

Growth experiments. Bacterial cultures were grown up to saturation in 3 ml of PS medium to obtain a preinoculum. The optical density of preinoculum from each culture was adjusted to an OD_{600} of 0.6 by dilution with PS medium. The preinoculum (0.2%, vol/vol) was added to PS medium under iron-limited or iron-supplemented conditions and grown at 28°C. For growth under iron-limiting conditions, DP and DFX were added to PS medium at different concentrations. Iron supplementation of PS medium was achieved by adding different concentrations of either $FeSO_4$ or ferric chloride ($FeCl_3$). Growth curves were obtained by monitoring a change in the OD_{600} over a period of 60 h. To determine growth yields, 0.3% of preinoculum (prepared as indicated above) was added, cultures were grown at 28°C for 48 h, and the number of CFU/ml of culture was determined by dilution plating on PSA medium. After 4 to 5 days, colonies were counted, and the results are expressed as means ± standard deviations (SD) of the log CFU/ml at 0 h and 48 h.

Siderophore supplementation bioassay. The ability of a siderophore to enhance growth of *X. oryzae* pv. oryzae strains under iron-limiting conditions was assessed using a siderophore supplementation bioassay. Spent culture supernatant of strain BXO43, grown to stationary phase in PS medium containing 100 μM DP (PS–100 μM DP medium), was used as a source of native siderophore. These culture supernatants were passed through 0.22-μm-pore-size filters (Millipore) to make them cell free. Siderophore activity in the spent supernatant was confirmed in a CAS assay by spotting 100 μl on a PSA-CAS plate and scoring for the appearance of an orange-yellow halo. Bioassay tubes contained 3 ml of PS–100 μM DP medium and ~10^6 CFU of selected *X. oryzae* pv. oryzae strains (i.e., BXO2211, BXO2231, and BXO2233). Tubes were supplemented with the following: 0.5 ml of the supernatant of the BXO43 strain grown in iron-limited or iron-supplemented medium, 0.5 ml of a culture supernatant of BXO2211 (*xssE* mutant) grown in PS medium, 120 μM $FeSO_4$, 120 μM $FeCl_3$, 50 μM DFX, 50 μM DHBA, and 50 μM ferrichrome (FCR). The growth yield of the *X. oryzae* pv. oryzae strains under the above-mentioned conditions was determined after 48 h and is expressed as log CFU/ml.

Virulence assay on rice plants. Forty-day-old greenhouse-grown rice plants of the susceptible rice cultivar Taichung Native-1 (TN-1) were inoculated by clipping leaf tips with sterile scissors dipped in cultures of PS-grown *X. oryzae* pv. oryzae strains resuspended in sterile double-distilled water (10^8 CFU/ml) (32). Lesion lengths were measured at regular intervals. In each experiment, 15 leaves were inoculated, and the values are presented as mean lesion lengths and standard deviations.

Reisolation of bacteria from rice leaves and revertant identification. Infected leaves were surface sterilized by being dipped in 1% (vol/vol) sodium hypochlorite (Loba Chemie) for 1 min and washed three times in distilled water. The leaves were cut at the leading edge of the lesion and dipped in 1 ml of sterile water for 5 min. Bacteria that exuded from the cut edge of the leaf were isolated by plating for individual colonies on PSA. These colonies were patched on PSA plates containing kanamycin, and the *feoB*$^+$ revertants were identified as kanamycin-sensitive colonies. The kanamycin-sensitive colonies were patched on PSA-CAS plates for assessing the siderophore production phenotype.

Histochemical staining of infected rice leaves. Rice leaves infected with GUS-marked strains were stained to determine β-glucuronidase activity, 12 days after infection, with 1 mM 5-bromo-4-chloro-3-indolyl β-D-glucuronide (X-Gluc, Sigma) in GUS assay buffer (50 mM sodium dihydrogen phosphate [pH 7.0] 10 mM EDTA, 0.1% Triton X-100, 0.1% sodium lauryl sarcosine, and 10 mM β-mercaptoethanol). Penetration of X-Gluc into leaves was facilitated by vacuum infiltration of leaves in assay buffer containing X-Gluc for 1 h, prior to incubation at 37°C. Destaining was performed by incubating stained leaves in absolute alcohol for 72 h at 37°C. Leaves were then observed under a compound microscope (Leica).

RESULTS

Sequence analysis of *X. oryzae* pv. oryzae *feoABC* operon. The genome of *X. oryzae* pv. oryzae KACC10331 strain (36) has a homolog of the *E. coli feoABC* operon. As in *E. coli*, the stop codon of the *X. oryzae* pv. oryzae *feoA* gene overlaps with the start codon of *feoB*, and the stop codon of *feoB* overlaps with the start codon of *feoC*, suggesting that these genes are co-operonic and translationally coupled (Fig. 1A). The *feoB* gene of *X. oryzae* pv. oryzae encodes a protein of 621 amino acids that has 29% identity and 45% similarity to *E. coli* FeoB. The N-terminal one-third of *X. oryzae* pv. oryzae FeoB is hydrophilic while the C terminus is hydrophobic and predicted to have 10 transmembrane α-helices. As in *E. coli*, the *X. oryzae* pv. oryzae FeoB protein contains four G protein signature sequences. All four well-defined sequence motifs, G1 (residues 16 to 23), G2 (residues 42 to 44), G3 (residues 63 to 66), and G4 (residues 128 to 131), were found in the N-terminal region of *X. oryzae* pv. oryzae FeoB. In *X. oryzae* pv. oryzae, the genes *feoA* and *feoC* encode two small proteins of 82 and 84 amino acids, respectively. A putative Fur binding site was identified upstream of the *X. oryzae* pv. oryzae *feoA* coding region (Fig. 1C), which contained 10/19 residues conserved in the *E. coli* Fur-box consensus sequence (GATAATGATAATCATTATC) (51) and 13/19 residues conserved in the *X. campestris* pv. campestris Fur-box consensus sequence (AATGAGAATCATTCTC ATT) (7). This suggests that, as in *E. coli*, expression of the *X. oryzae* pv. oryzae *feoABC* operon is regulated in response to levels of intracellular iron. Interestingly, the Fur binding site overlaps with a Clp (CAP-like protein) binding site. The Clp binding site of *X. campestris* pv. campestris is TGTGA-N6-TCACA (27). The

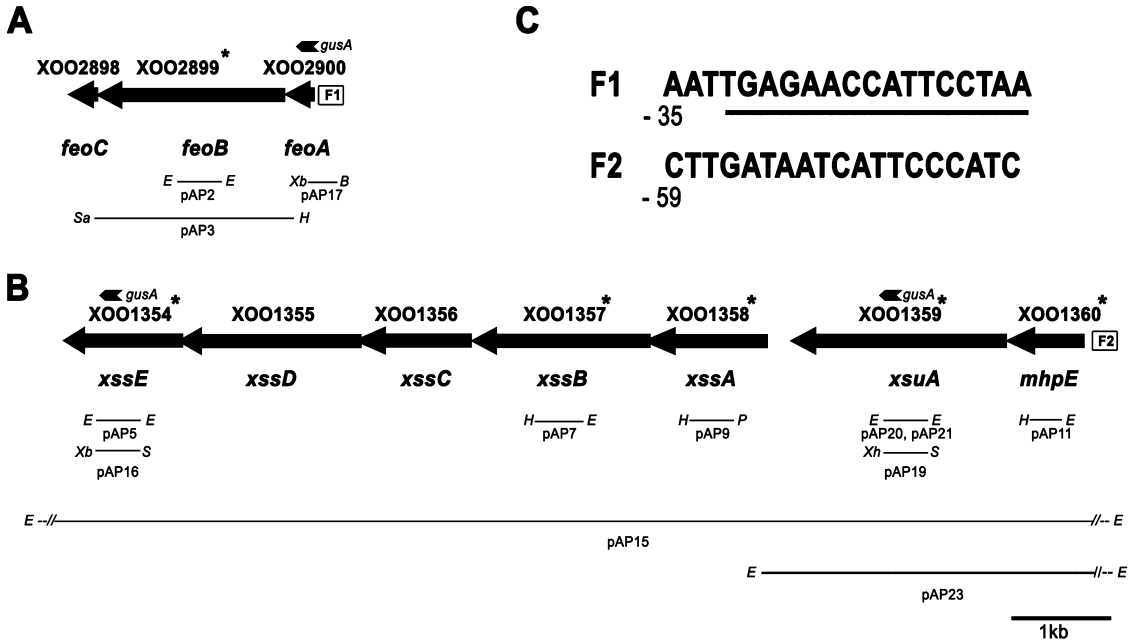

FIG. 1. Genetic organization of *X. oryzae* pv. oryzae loci encoding functions involved in iron acquisition. Solid arrows represent open reading frames. Gene numbers are as specified by Lee et al. (36). (A) The *X. oryzae* pv. oryzae *feoABC* operon and cloned fragments. F1 represents a putative Fur binding site (FBS). (B) Organization of the *X. oryzae* pv. oryzae *xss* gene cluster involved in biosynthesis, export, and utilization of siderophore, including *xss* (*Xanthomonas* siderophore synthesis) genes, *xsuA* (*Xanthomonas* siderophore utilization) gene, and the *mhpE* gene encoding 4-hydroxy 2-oxovalerate aldolase. F2 represents an FBS. (C) Sequences of F1 and F2. The numbers indicate position of the FBS relative to translational start site, and the underlined sequence in F1 represents a putative Clp (CAP-like protein) regulator binding site. Thin lines represent cloned genomic regions, internal fragments of genes, and promoter regions that were used for complementation analysis, construction of mutations, and chromosomal GUS reporter fusions. Small arrowheads marked with *gusA* represent the positions of GUS reporter fusions. Gene numbers with asterisks indicate that the mutations in the corresponding genes were generated in this study. Restriction sites are abbreviated as follows: E, EcoRI; H, HindIII; Xb, XbaI; B, BamHI; Sa, SacI; P, PstI; S, SpeI; Xh, XhoI.

putative Clp binding site upstream of the *feoA* coding region (Fig. 1C) has a match of 6/10 with the invariant residues in the *X. campestris* pv. campestris Clp binding site. Clp is homologous to the cyclic AMP (cAMP) nucleotide receptor protein Crp of *E. coli* and regulates several important biological functions of *X. campestris* pv. campestris (27). The *feoABC* locus is almost identical in all other xanthomonads that have been sequenced to date.

Transcriptional organization of *feoABC* genes. RT-PCR demonstrated that *X. oryzae* pv. oryzae *feoA*, *feoB*, and *feoC* genes are cotranscribed under iron-supplemented and iron-limiting conditions (Fig. 2A to C). A chromosomal transcriptional fusion strain (BXO2230; *feo*::*gusA*) was constructed such that the promoter of the *feoABC* operon is fused to a *gusA* reporter while retaining a functional copy of *feoABC* with its native promoter. When this strain was assayed for β-glucuronidase activity under iron-limiting conditions imposed by the addition of either 25 μM, 50 μM, or 100 μM 2,2′-dipyridyl ([DP] an iron chelator) to the PS medium, a gradual increase in β-glucuronidase activity was observed, indicating the induction of expression of the *feoABC* operon following iron depletion (Fig. 2D). The level of expression of the *feo*::*gusA* fusion is almost the same in either PS medium or PS medium supplemented with 25 μM or 100 μM ferrous sulfate. Overall, the RT-PCR data and GUS reporter assays indicate that, although expression of *feoABC* operon is induced by iron limitation, a basal level is observed even under high-iron conditions.

***X. oryzae* pv. oryzae *feoB* mutant overproduces siderophores and exhibits growth deficiency under iron-limiting conditions.** The *X. oryzae* pv. oryzae *feoB* mutant (strain BXO2201) overproduces siderophores on peptone-sucrose agar and chrome azurol S (PSA-CAS) medium. The wild-type strain BXO43 does not produce siderophores under these conditions (Fig. 3A). Introduction of the *feoB* gene on a complementing plasmid (BXO2206), but not the empty vector (BXO2204), abolishes the siderophore overproduction phenotype of the *feoB* mutant. The overproduction of siderophores by the *feoB* mutant might be a compensatory measure to overcome the loss of *feoB* function.

BXO43, BXO2201, and BXO2206 were grown in PS medium, with and without addition of DP. All three strains grew equally well in PS medium (Fig. 4A). There was no significant effect of the addition of DP (25 μM or 50 μM) on growth of either BXO43 or BXO2206. In contrast, BXO2201 displayed a significant decrease in growth as the concentration of DP increased (Fig. 4B and C). At 100 μM DP, growth of BXO2201 was almost negligible (Fig. 4D). The *feoB* mutant also exhibited a growth deficiency in PS medium containing deferoxamine mesylate (a specific ferric iron chelator) (data not shown). Taken together, these data suggested that FeoB is required for growth of *X. oryzae* pv. oryzae in low-iron medium.

Identification of a siderophore-biosynthetic gene cluster in *X. oryzae* pv. oryzae. By employing the Arnow and Csaky tests

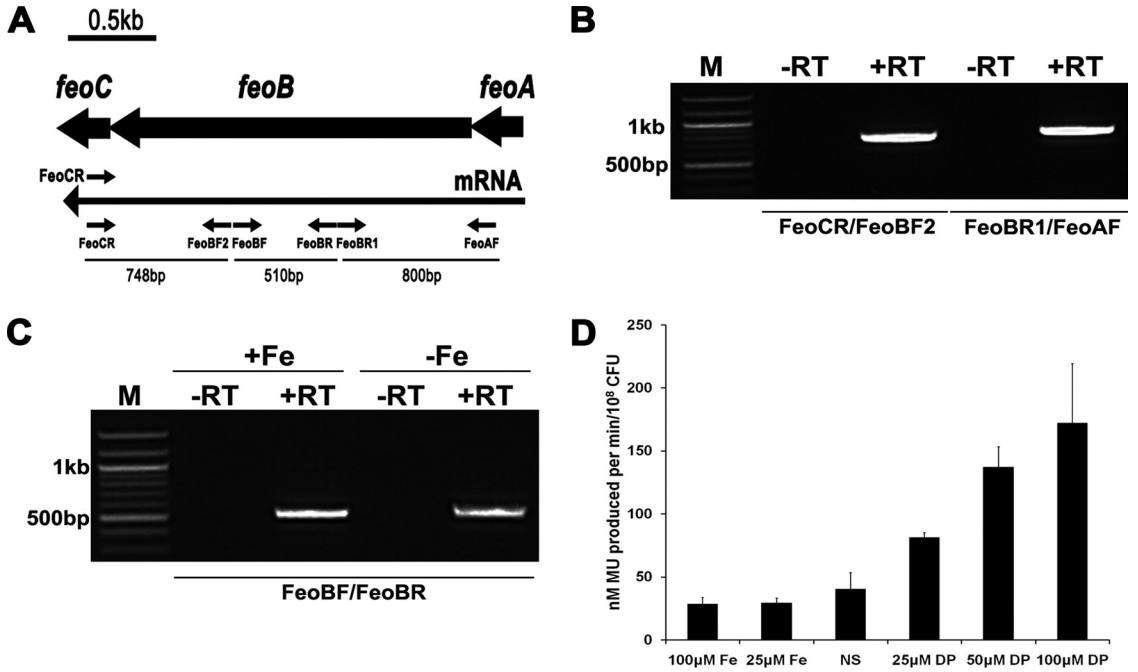

FIG. 2. Operon mapping and expression analysis of *X. oryzae* pv. oryzae *feo* operon. (A) Solid arrows represent the *feoA*, *feoB*, and *feoC* ORFs. The long arrow represents the *feoABC* mRNA. The small arrows denote the positions and directions of primers used in RT-PCR. FeoCR primer was used in cDNA first-strand synthesis while FeoCR as well as other primers were used in subsequent PCRs. Lengths of expected PCR products are also shown for every primer pair. (B) RT-PCR analysis indicates that *feoABC* genes are cotranscribed as a single mRNA. The FeoBF2/FeoCR and the FeoAF/FeoBR1 primer pairs yield the expected 748-bp and 800-bp fragments, respectively. (C) The *feoB* transcript is present under iron-supplemented (100 μM $FeSO_4$; +Fe) and iron-limited (100 μM DP, an iron chelator; −Fe) growth conditions. The expected 510-bp fragment is amplified by the FeoBF/FeoBR primer pair under both conditions. Lanes: −RT, without reverse transcriptase; +RT, with reverse transcriptase; M, 100-bp DNA molecular markers. (D) Expression of *feo*::*gusA* transcriptional fusion. The *feo*::*gusA* strain (BXO2230; $FeoB^+$) was grown under either iron-supplemented (different concentrations of $FeSO_4$; Fe), or iron-limited (different concentrations of DP) conditions or with no supplementation (NS). β-Glucuronidase activity is represented as nanomoles of methyl-umbelliferone (MU) produced/minute/10^8 CFU of bacteria. Data represent means ± standard deviations of values from three independent experiments.

(52), we were able to determine that the siderophore produced by *X. oryzae* pv. oryzae is not of either the catecholate or hydroxamate type (data not shown). This suggested that the *X. oryzae* pv. oryzae siderophore might be of the α-hydroxy carboxylate type. We found that *X. campestris* pv. campestris strain ATCC 33913 and *X. axonopodis* pv. citri (a pathogen of citrus) strain 306 (20) have a homolog of the *Vibrio parahaemolyticus pvs* locus, which encodes five genes involved in the biosynthesis of vibrioferrin, an α-hydroxy carboxylate-type of siderophore, and the *pvuA* gene, which is involved in vibrioferrin uptake (67). Degenerate oligonucleotide primers (Table 3) were used to amplify internal fragments of all six genes from the genome of *X. oryzae* pv. oryzae strain BXO43, and sequencing confirmed the identity of these genes. During the course of this work, the genome sequence of *X. oryzae* pv. oryzae strain KACC10331 (36) was released, and we found that the genes XOO1354-XOO1359 are homologous to *pvsABCDE* and *pvuA* genes. In addition, we observed that the stop codon of XOO1360 overlaps with the start codon of XOO1359. We named this gene cluster *xss* (*Xanthomonas* siderophore synthesis) (Fig. 1B), and we designated open reading frames (ORFs) XOO1354-XOO1359 *xssE*, *xssD*, *xssC*, *xssB*, *xssA*, and *xsuA* while ORF XOO1360 was named *mhpE* (encodes 4-hydroxy 2-oxovalerate aldolase) based on its homology. The similarity/identity of XOO1354-XOO1360 to the genes involved in biosynthesis/uptake of siderophores in other organisms is shown in Table 5.

The *xssE* gene product is closely related to pyridoxal 5′-phosphate (PLP)-dependent decarboxylase family enzymes and also to diaminopimelate decarboxylases (LysA) which are predicted to be involved in siderophore biosynthesis. The protein products encoded by *xssD* and *xssB* belong to type A and B NRPS-independent siderophore (NIS) synthetases and showed 25% and 24% identity (39% and 39% similarity) to IucA and IucC proteins of *E. coli*, respectively, which catalyze amide bond formation during aerobactin biosynthesis in *E. coli* (13, 41). The *xssA* gene product is homologous to a family of proteins which include D-Ala-D-Ala ligase enzymes. The *mhpE* gene encodes a 4-hydroxy 2-oxovalerate aldolase protein which belongs to the HpcH/HpaI aldolase/citrate lyase family. This enzyme acts on 4-hydroxy 2-oxovalerate to release pyruvate and acetaldehyde (37). The *xssC* gene is predicted to encode a cytoplasmic membrane protein (as determined by PSORTb) having a membrane spanning region comprised of 12 α-helices and is homologous to multidrug efflux pumps of the major facilitator superfamily (MFS) of proteins. MFS proteins facilitate the transport of a variety of substrates across the cytoplasmic membrane (53). XssC is the *X. oryzae* pv. oryzae homolog of PvsC, which functions as an exporter of vibrioferrin (68). The *xsuA* gene is predicted to encode a 713-amino-acid-

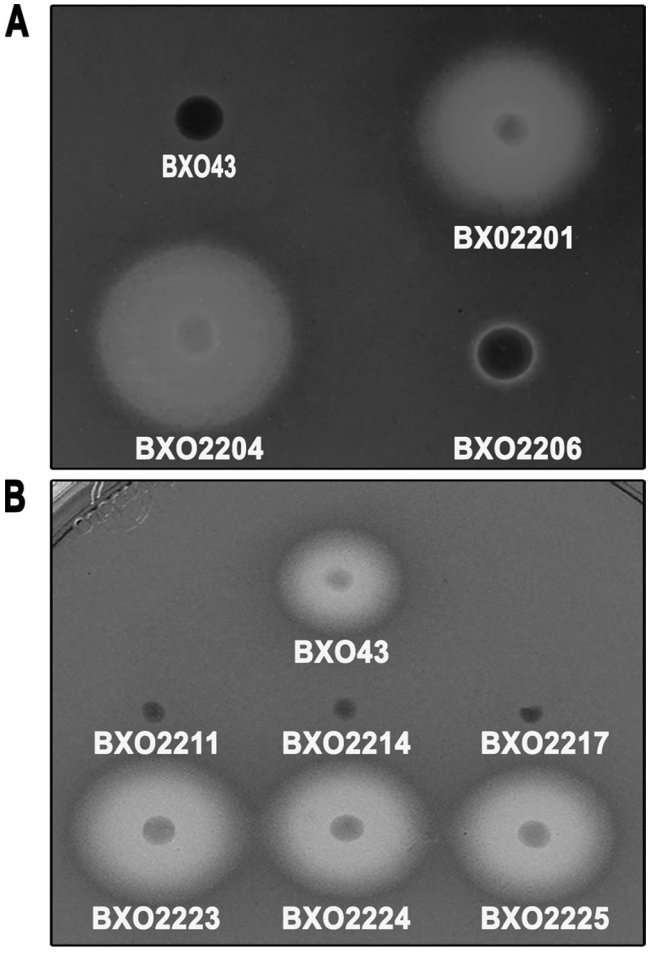

FIG. 3. Siderophore production phenotype of *X. oryzae* pv. oryzae strains with mutations in genes involved in iron acquisition. Siderophore production is assayed as the presence of a halo around colonies growing on PSA-CAS medium. (A) An *X. oryzae* pv. oryzae *feoB* mutant overproduces siderophores. The *X. oryzae* pv. oryzae strains used are BXO43 (wild-type strain), BXO2201 (*feoB1*::pK18*mob*), BXO2204 (BXO2201/pHM1; vector control), and BXO2206 (BXO2201/pAP3; complemented strain). The pAP3 plasmid carries the cloned *X. oryzae* pv. oryzae *feoB* gene. (B) Mutations in *xss* genes result in a deficiency for siderophore production. Siderophore production was assessed by growth on PSA-CAS medium containing 100 μM DP. The *X. oryzae* pv. oryzae strains used are BXO43 (wild-type strain), BXO2211 (*xssE1*::pK18*mob*), BXO2214 (*xssB1*::pK18*mob*), BXO2217 (*xssA1*::pK18*mob*), BXO2223 (BXO2211/pAP15;, complemented strain), BXO2224 (BXO2214/pAP15; complemented strain), and BXO2225 (BXO2217/pAP15; complemented strain). The pAP15 cosmid contains the entire *xss* gene cluster of *X. oryzae* pv. oryzae. Plasmid pK18*mob* has an outreading *lacZ* promoter for transcribing downstream genes.

long outer membrane-located (as determined by PSORTb) protein that is homologous to PvuA, the ferric vibrioferrin receptor (24). These similarities suggest that the *xss* gene cluster is involved in biosynthesis, export, and uptake of a vibrioferrin kind of siderophore. Overlapping start and start codons were present between all genes of the *xss* cluster except *xssA* and *xsuA*, which are separated by 235 bp (Fig. 1B). This suggested that this gene cluster of ~10.5 kb might be transcriptionally organized as an operon. A putative Fur binding site was identified upstream of the *X. oryzae* pv. oryzae *mhpE* coding region (Fig. 1C), which contained 12/19 residues conserved in *E. coli* Fur-box consensus sequence (51) and 14/19 residues conserved in *X. campestris* pv. campestris Fur-box consensus sequence (7).

Although the *xss* gene cluster is present in the genomes of all other xanthomonads that have been sequenced to date, this gene cluster is not present in the genomes of the closely related *Xylella fastidiosa* (6) and *Stenotrophomonas maltophilia* (18). In *X. oryzae* pv. oryzae and other xanthomonads, the *xss* gene cluster is adjacent to the vitamin B_{12}-biosynthetic gene cluster. The XOO1362 (a cation-proton antiporter) and XOO1337 (*clpB*) genes flank this genomic region. Interestingly, BLAST N analysis reveals that the *S. maltophilia* genes Smlt3726 (homolog of XOO1362) and Smlt3732 (homolog of XOO1337) are present near each other with a few *Stenotrophomonas*-specific genes and the *metB* gene (encodes for cystathionine gamma-synthase) being located between them. The colinearity at this locus between the *Xanthomonas* and *Stenotrophomonas* genomes suggests that the *xss* gene cluster was either introduced into this locus at an early stage in the *Xanthomonas* lineage or that it was deleted from the *Stenotrophomonas* lineage. However, *S. maltophilia* has a gene cluster that is homologous to a gene cluster involved in biosynthesis of enterobactin, a catecholate-type of siderophore produced by *E. coli* (60).

The *xss* genes are part of an operon which is induced by iron limitation. RT-PCR demonstrated that *xssA*, *xssB*, *xssC*, *xssD*, *xssE*, *xsuA*, and *mhpE* genes are cotranscribed as a polycistronic mRNA whose expression is controlled in response to iron availability (Fig. 5A and B). The expression of an *xssE*::*gusA* transcriptional fusion (BXO2229) was analyzed under iron-supplemented and iron-limiting conditions. High levels of β-glucuronidase activities were observed under iron-depleted conditions (addition of different concentrations of DP) (Fig. 5C). A very low basal level of expression was observed for the *xssE*::*gusA* fusion during growth in either PS medium or under iron-supplemented conditions.

In order to exclude the possibility that there is a promoter between the *xssA* and *xsuA* genes, a nonpolar mutant (BXO2235; *xsuA2*::pK18*mob*) and a polar mutant (BXO2236; *xsuA3*::pK18*mob*) of the *xsuA* gene were constructed as described in Materials and Methods. A polar mutation in the *xsuA* gene blocked siderophore biosynthesis while a nonpolar mutation did not affect the production of siderophore on PSA-CAS-DP medium (see Fig. 8A). Moreover, BXO2235 produces siderophore on PS medium, a condition in which BXO43 does not produce siderophore, indicating that the *lacZ* promoter of the integrated vector pK18*mob* is driving the transcription of *xssABCDE* genes in this strain. These data suggest that there is no relevant promoter in the intergenic region between *xssA* and *xsuA* and that a promoter present upstream of *mhpE* drives transcription of the *xss* operon.

***xssA*, *xssB*, and *xssE* mutants are siderophore deficient and exhibit growth deficiency under low-iron conditions.** Nonpolar mutations were created by plasmid integration in the *xssE*, *xssB*, *xssA*, and *mhpE* genes as described in Materials and Methods, and the generated mutants were named as BXO2211, BXO2214, BXO2217, and BXO2220, respectively. The ability of these mutants to produce siderophores was assessed on PSA-CAS-DP plates. In contrast to BXO43, mutants BXO2211, BXO2214, and BXO2217 failed to produce a halo

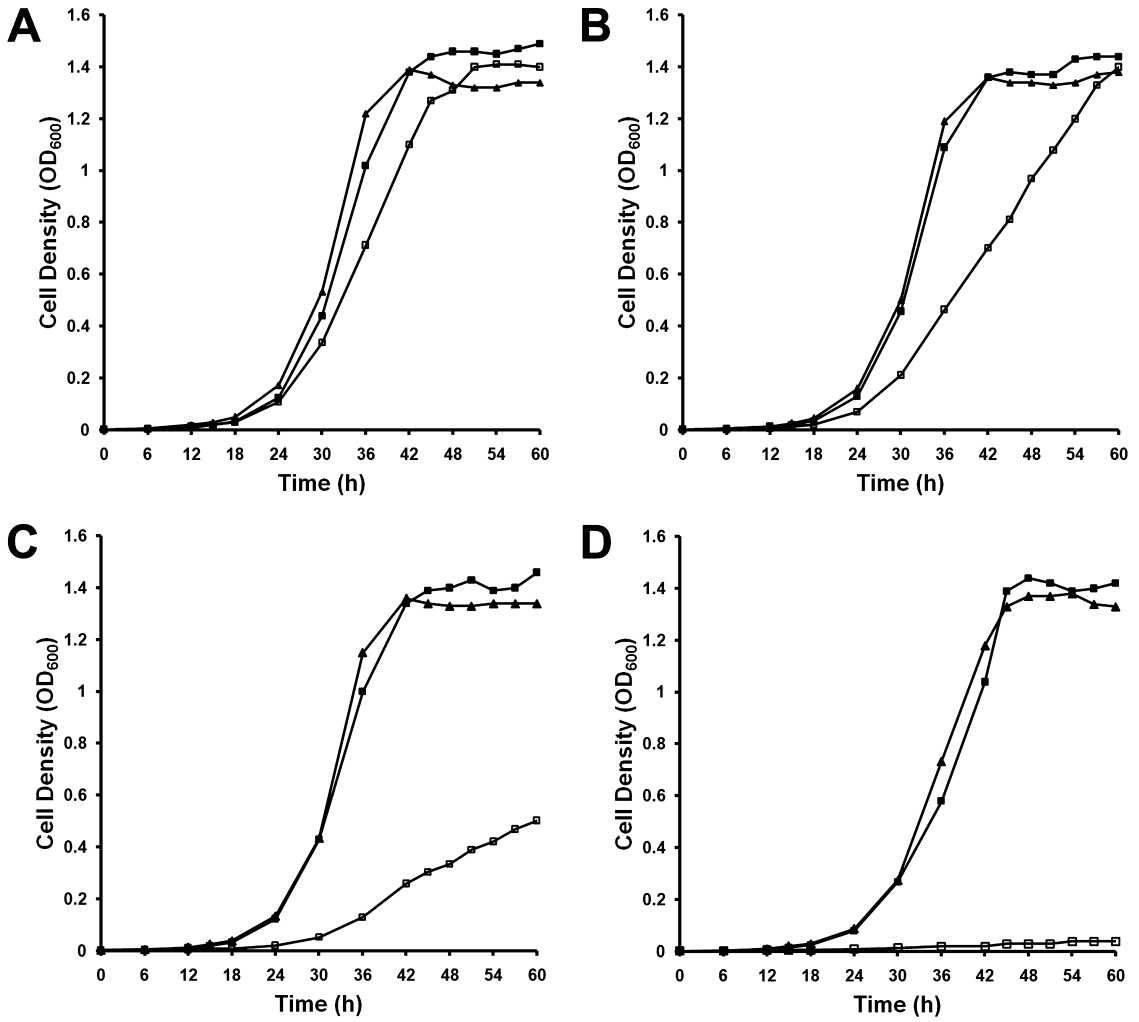

FIG. 4. A *feoB* mutant of *X. oryzae* pv. oryzae is deficient for growth under conditions of iron limitation. Wild-type BXO43 (filled squares), *feoB* mutant (*feoB1*::pK18*mob*; open squares), and complemented strain BXO2206 (BXO2201/pAP3; filled triangles) were grown in PS medium (A) PS supplemented with 25 μM DP (B) PS medium with 50 μM DP (C), and PS medium with 100 μM DP (D). Bacterial growth was monitored by determining the OD_{600}. The results were reproducible in an independent experiment.

on PSA-CAS-DP medium (Fig. 3B), indicating that these mutants are impaired in siderophore production. We introduced a cosmid clone (pAP15) containing the entire *xss* gene cluster to these mutants to get complemented strains BXO2223 (for the *xssE* mutant), BXO2224 (for the *xssB* mutant), and BXO2225 (for the *xssA* mutant). These complemented strains produced wild-type levels of siderophore on PSA-CAS-DP medium (Fig. 3B). Overall, these results indicate that mutation of the *xssA*, *xssB*, and *xssE* genes affects the ability of *X. oryzae* pv. oryzae to produce siderophore, a phenotype which can be restored by complementation in *trans*. However, although it is less likely, there is a possibility that the siderophore-deficient phenotype of the *xssA* and *xssB* mutants is not due to gene inactivation but to overexpression of downstream genes caused by the nonpolar mutation. The *mhpE* mutant (BXO2220) showed no defect in siderophore production on PSA-CAS-DP medium (data not shown), indicating that this gene is not essential for siderophore biosynthesis in *X. oryzae* pv. oryzae.

In PS medium, no significant difference in growth yields was observed between the wild-type and the BXO2211, BXO2214, BXO2217, and BXO2220 strains. When these mutants were cultured in PS–100 μM DP medium (iron-limiting conditions), the siderophore-deficient mutants (BXO2211, BXO2214, and BXO2217) exhibited a severe deficiency for growth (Fig. 6A). The siderophore-proficient strains, BXO43, BXO2220, and BXO2223, grew quite well under these conditions (Fig. 6). The siderophore-deficient mutants (BXO2211, BXO2214, and BXO2217) also exhibited a growth deficiency in PS medium containing deferoxamine mesylate (a specific ferric iron chelator) (data not shown). These results indicate that the *xssA*, *xssB*, and *xssE* genes are essential for siderophore biosynthesis and growth under low-iron conditions.

Siderophore restores the growth of the *xssE* mutant in iron-deficient medium. We examined the ability of siderophore to promote the growth of BXO2211 (*xssE* mutant) on PS–100 μM DP medium by supplementation with culture supernatants (taken as source of native siderophore) of a BXO43 strain grown PS–100 μM DP medium. The presence of siderophore

TABLE 5. Homologous proteins for functions encoded in the *xss* gene cluster of *X. oryzae* pv. oryzae

X. oryzae pv. oryzae protein		Putative homologue		E value[a]	I/S[b]
Name (length [aa])	Function	Name and/or function (% match in length)	Bacterium		
XssE (426)	Diaminopimelate decarboxylase/ PLP-dependent decarboxylase[c]	PvsE; vibrioferrin biosynthesis (86)	*Vibrio parahaemolyticus*	2e-111	53/67
		AcsE; achromobactin biosynthesis (87)	*Erwinia chrysanthemi*	3e-80	45/58
		Siderophore synthesis decarboxylase (87)	*Ralstonia solanacearum*	2e-85	45/58
		SbnH; staphyloferrin B biosynthesis (88)	*Staphylococcus aureus*	3e-85	40/58
XssD (591)	Type A siderophore synthetase	PvsD; vibrioferrin biosynthesis (94)	*Vibrio parahaemolyticus*	5e-126	43/57
		Siderophore biosynthetic protein (73)	*Ralstonia solanacearum*	e-40	31/46
		AcsD; achromobactin biosynthesis (97)	*Erwinia chrysanthemi*	7e-53	29/44
		RhbC; rhizobactin biosynthesis (77)	*Sinorhizobium meliloti*	8e-37	28/41
		SbnE; staphyloferrin B biosynthesis (81)	*Staphylococcus aureus*	2e-40	27/43
		IucA; aerobactin biosynthesis (82)	*Escherichia coli*	3e-30	25/39
XssC (398)	Major facilitator superfamily multidrug efflux pump	PvsC; multidrug efflux pump homologue (100)	*Vibrio parahaemolyticus*	8e-73	43/58
XssB (600)	Type B siderophore synthetase	PvsB; vibrioferrin biosynthesis (95)	*Vibrio parahaemolyticus*	6e-120	44/58
		AcsA; achromobactin biosynthesis (66)	*Erwinia chrysanthemi*	3e-28	31/45
		LbtA; legiobactin biosynthesis (54)	*Legionella pneumophila*	7e-23	29/47
		SbnC; staphyloferrin B biosynthesis (64)	*Staphylococcus aureus*	3e-22	24/44
		IucC; aerobactin biosynthesis (50)	*Escherichia coli*	e-12	24/39
XssA (408)	D-Alanine-D-Alanine ligase/ATP-dependent amino acid ligase	PvsA; vibrioferrin biosynthesis (95)	*Vibrio parahaemolyticus*	e-92	45/60
XsuA (713)	TonB-dependent outer membrane receptor	PvuA; ferric vibrioferrin receptor (93)	*Vibrio parahaemolyticus*	2e-156	43/61
		FecA; ferric citrate outer membrane receptor (92)	*Escherichia coli*	2e-47	31/47
MhpE (253)	4-Hydroxy 2-oxovalerate aldolase	AcsB; achromobactin biosynthesis (93)	*Erwinia chrysanthemi*	e-32	36/53
		SbnG; staphyloferrin B biosynthesis (93)	*Staphylococcus aureus*	7e-32	35/52

[a] E values were obtained by using the BLAST algorithm.
[b] I/S, % identity/% similarity.
[c] PLP, pyridoxal 5′-phosphate.

in the supernatant of BXO43 grown in PS–100 μM DP medium was confirmed by spotting supernatants on PSA-CAS plates. The addition of culture supernatant of the BXO43 strain enhanced the growth of BXO2211, resulting in a level of cell density similar to that observed in PS medium. Interestingly, cell-free supernatant of BXO43 culture grown in PS medium also promoted (~10-fold) the growth of BXO2211. This suggests that during growth in PS medium, BXO43 produces a slight amount of siderophore which can minimally enhance growth of the BXO2211 strain. However, this level of siderophore production was not detectable on PSA-CAS plates. In addition, supplementation with either $FeSO_4$ or $FeCl_3$ was equally efficient in restoring the growth of BXO2211 (Fig. 7). Restoration of growth of BXO2211 to the level that is observed in iron-sufficient medium by siderophore supplementation again confirmed that siderophore production is required for growth on low-iron medium. Importantly, supplementation with the culture supernatant of BXO2211 grown in PS medium did not promote growth of BXO2211.

As bacteria often can utilize exogenous siderophores that cannot be biosynthesized by them, the ability of BXO2211 to utilize three exogenous siderophores was tested. We used 2,3-dihydroxy benzoic acid, a catecholate type of siderophore, as well as ferrichrome and deferoxamine mesylate, two hydroxamate siderophores. These siderophores did not exhibit a growth-promoting activity on BXO2211 (Fig. 7).

The *xsuA* gene appears to be involved in siderophore uptake. In addition to the two *xsuA* mutants described above, a polar mutation in the *xsuA* gene was generated (as described in Materials and Methods) by integration of plasmid pVO155 to create the strain BXO2231 (*xsuA1*::pVO155). The siderophore production phenotype of the *xsuA* mutants was assessed on PSA-CAS-DP. BXO2231 and BXO2236 were found to be defective in siderophore production while BXO2235 was able to produce siderophores (Fig. 8A and Fig. 9A). The ability of the BXO2235 (*xsuA2*::pK18*mob*) mutant to produce siderophores indicated that *xsuA* is not essential for siderophore production and that the mutation in this strain is not polar on expression of downstream *xss* genes. The siderophore-deficient phenotype of the BXO2231 and BXO2236 strains indicated that, in these strains, the insertion mutation in the *xsuA* gene is polar on expression of downstream *xss* genes. In the BXO2231 background, a cosmid (pAP23) containing the *xsuA* gene, but devoid of *xss* genes, and another cosmid having the entire *xss* gene cluster including *xsuA* (pAP15) were mobilized to get complemented strains, BXO2233 and BXO2234, respectively. As expected, BXO2234 was able to produce siderophores, but BXO2233 was still defective for siderophore production (Fig. 9A).

Growth yield assays were performed for *xsuA* mutants under iron-limiting conditions imposed by the addition of 100 μM DP. Under these conditions all three mutants, BXO2231,

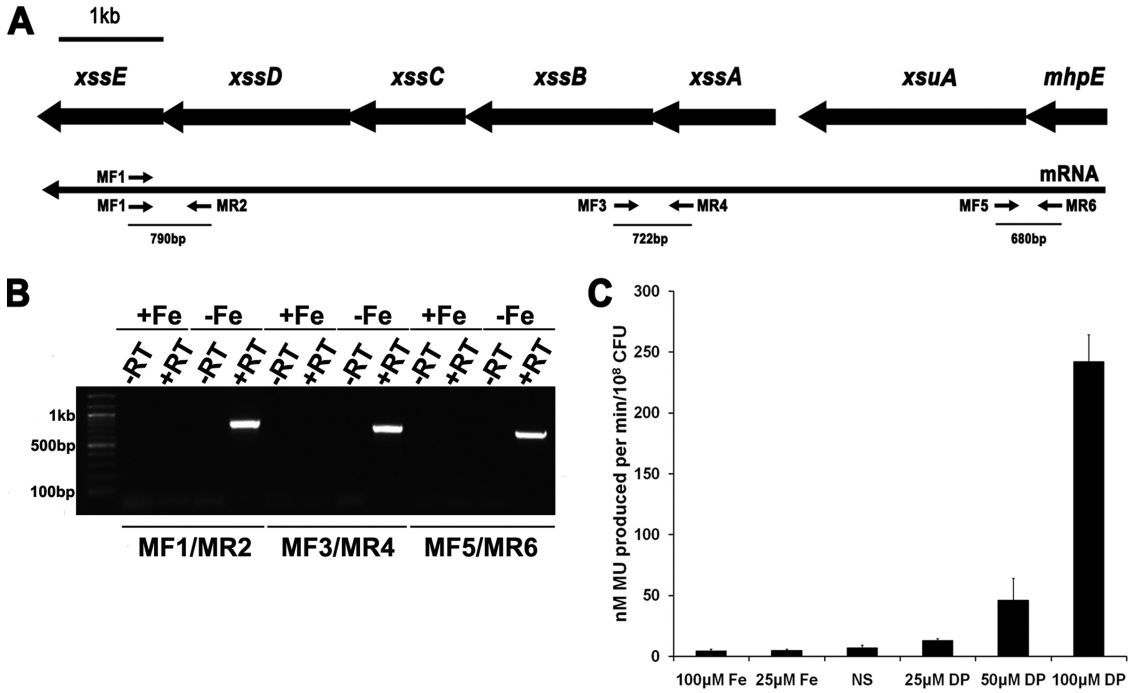

FIG. 5. Operon mapping and expression analysis of *xss* gene cluster of *X. oryzae* pv. oryzae. (A) Solid arrows represent the *xssABCDE*, *xsuA*, and *mhpE* ORFs. The long arrow represents the mRNA transcript. The small arrows denote the positions and directions of primers used in RT-PCR. MF1 primer was used in cDNA first-strand synthesis, and MF1 as well as other primers were used in subsequent PCRs. Lengths of expected PCR products are also shown for every primer pair. (B) Lanes contain RT-PCR products amplified from total RNA isolated from *X. oryzae* pv. oryzae cultures grown under iron-supplemented (+Fe; 100 μM $FeSO_4$) and iron-limiting (-Fe; 100 μM DP, an iron chelator) conditions as described in Materials and Methods. The primer pairs MF1/MR2, MF3/MR4, and MF5/MR6 yielded the expected DNA fragments of 790 bp, 722 bp, and 680 bp, respectively, exclusively from mRNA templates under iron-limiting conditions. No amplification was observed from mRNA templates expressed under iron-supplemented conditions. Lanes −RT and +RT, without and with reverse transcriptase, respectively; lane M, 100-bp DNA molecular marker. (C) Transcriptional analysis of *xssE* gene involved in siderophore biosynthesis carried out with GUS reporter strain BXO2229 (*xssE2*::*gusA*). BXO2229 was grown under either iron-supplemented (different concentrations of $FeSO_4$; Fe) or iron-limited (different concentrations of [DP]) conditions or with no supplementation (NS). β-Glucuronidase activity is represented as the nanomoles of methylumbelliferone produced/minute/10^8 CFU of bacteria. Data represent mean ± standard deviation of values from three independent experiments.

BXO2235, and BXO2236, were severely deficient for growth compared with wild-type BXO43. These strains grew as well as BXO43 in PS medium (Fig. 8B and 9B). The growth deficiency of the BXO2235 mutant on low-iron medium, in spite of the mutant's proficient siderophore production, is consistent with the possibility that *xsuA* encodes a siderophore receptor. To investigate the ability of *xsuA* mutants to utilize native siderophore, supplementation was carried out with spent culture supernatants of a BXO43 strain grown on PS—100 μM DP medium. Upon supplementation with the culture supernatant of BXO43, a BXO2211 (*xssE* mutant) strain was able to grow in PS—100 μM DP medium, but the BXO2231 was unable to grow under these conditions (Fig. 9C). This suggested that BXO2231 is unable to utilize the siderophore present in the culture medium, a phenotype that is indicative of a deficiency in siderophore uptake. Introduction of the plasmid pAP23 (which carries only the *xsuA* gene) restores the ability of the BXO2231 strain to grow on PS—100 μM DP medium supplemented with culture supernatant of BXO43 (Fig. 9D, BXO2233). As expected, introduction of the cosmid pAP15 (which carries the entire *xss* gene cluster including *xsuA*) into BXO2231 also restores the ability of this strain to grow on PS—100 μM DP medium (Fig. 9D, BXO2234).

***feoB* mutant is virulence-deficient while siderophore-deficient mutants are virulence proficient.** The virulence phenotypes of BXO43 (wild-type strain), BXO2201 (*feoB* mutant), BXO2204 (BXO2201/pHM1; control), and BXO2206 (BXO2201/pAP3, which carries *feoB* for complementation) were determined by assessing lesion lengths in rice 7 and 14 days after inoculation (as described in Materials and Methods). At both time points, the BXO2201 and BXO2204 strains showed significantly reduced lesions compared to lesions produced by BXO43 and BXO2206 (Fig. 10A). However, we observed that the BXO2201 and BXO2204 strains produced slightly elongated lesions at 14 days after inoculation compared to lesions observed at 7 days after inoculation. To determine whether this increase in lesion length was caused by the presence of any $feoB^+$ revertants *in planta*, *X. oryzae* pv. oryzae cells were reisolated (as described in Materials and Methods) from leaves infected with BXO2201. Reisolated bacteria were found to exhibit the wild-type phenotype with respect to siderophore production; i.e., they did not produce siderophore on PSA medium but produced siderophore on PSA-DP medium (data not shown). Also, these bacteria were kanamycin susceptible, suggesting that they arose after loss of the integrated plasmid. Taken together, these results remarkably illustrate the impor-

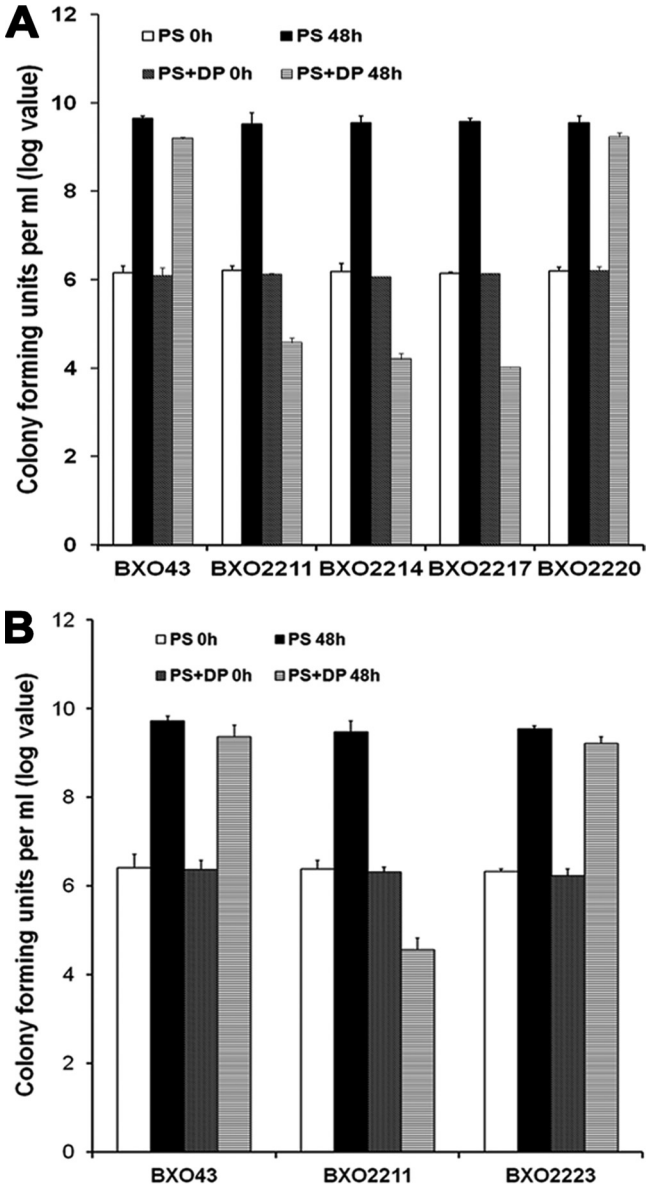

FIG. 6. Mutations in *xss* genes affect growth of *X. oryzae* pv. oryzae in iron-limited medium. Cell numbers were estimated in *X. oryzae* pv. oryzae cultures grown in PS medium and PS medium containing 100 μM DP (an iron chelator) at 0 h and after 48 h of growth. Data are the mean log CFU values ± standard deviations from three independent experiments. (A) Mutations in *xss* genes, but not the *mhpE* gene, result in a severe growth deficiency under iron-limiting conditions. Strains are BXO43 (wild-type strain), BXO2211 (*xssE1*::pK18*mob*), BXO2214 (*xssB1*::pK18*mob*), BXO2217 (*xssA1*::pK18*mob*), and BXO2220 (*mhpE1*::pK18*mob*). (B) Genetic complementation restores growth of a *xssE1*::pK18*mob* mutant under iron-limiting medium. Strains are BXO43 (wild-type strain), BXO2211 (*xssE1*::pK18*mob*), and BXO2223 (BXO2211/pAP15). The pAP15 cosmid contains the entire *xss* gene cluster of *X. oryzae* pv. oryzae. The pAP15 cosmid also corrects the growth deficiency of the *xssB* and *xssA* mutants on iron-limited medium (data not shown). Plasmid pK18*mob* has an outreading *lacZ* promoter for transcribing downstream genes.

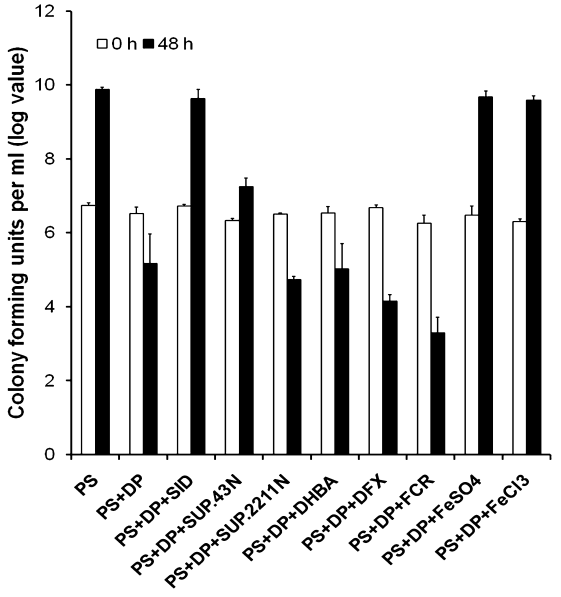

FIG. 7. Siderophore supplementation bioassays. Cell numbers (log value) were estimated at 0 h and after 48 h of growth in cultures of a siderophore-deficient *X. oryzae* pv. oryzae mutant (strain BXO2211; *xssE1*::pK18*mob*) grown in PS medium, PS–100 μM DP medium, and PS–100 μM DP medium with supplements. The different supplements used are as follows: SID, cell-free supernatant of a saturated culture of wild-type *X. oryzae* pv. oryzae strain BXO43 grown in iron-deficient medium (PS–100 μM DP medium; SUP.43N, cell-free supernatant of a saturated culture of BXO43 grown in PS medium; SUP.2211N, cell-free supernatant of a saturated culture of the siderophore-deficient mutant BXO2211 grown in PS medium; 50 μM DHBA; 50 μM DFX; 50 μM FCR; 120 μM $FeSO_4$; and 120 μM $FeCl_3$. The culture volume was 3 ml, of which 0.5 ml was cell-free culture supernatant in applicable experiments. The results from three independent experiments are expressed as means ± standard deviations.

tance of FeoB for virulence of *X. oryzae* pv. oryzae on rice. In contrast, an *xssE* mutant (BXO2211) was found to be as virulence proficient as the wild-type strain BXO43 (Fig. 10B). An *xssB* mutant (BXO2214), *xssA* mutant (BXO2217), and *xsuA* mutant (BXO2231) were also as virulence proficient as BXO43 (data not shown). These observations indicate that siderophore-mediated iron acquisition is not essential for *in planta* growth of *X.* oryzae pv. oryzae. Virulence proficiency of BXO2220 (data not shown) also indicated that the *mhpE* gene does not have a role in virulence of *X. oryzae* pv. oryzae.

***feoB* gene of *X. oryzae* pv. oryzae is expressed during *in planta* growth.** Rice leaves were inoculated with either BXO2230 (*feo*::*gusA*) or BXO2229 (*xssE*::*gusA*), and the leaves were stained for GUS expression 12 days after infection. As described above, the *feo*::*gus* fusion retains a wild-type copy of the *feo* operon under the control of its native promoter and is, hence, proficient for virulence. GUS activity was assessed by staining the infected leaves with the chromogenic substrate X-Gluc, as described in Materials and Methods. GUS staining (blue-green) was not detected in xylem vessels from leaves infected with either BXO43 (as a negative control) or BXO2229 (Fig. 11A and C), whereas GUS activity was detected in major longitudinal veins and minor longitudinal veins of rice leaves infected with BXO2230 (Fig. 11B, I and II, respectively). Bacteria were reisolated from rice leaves infected with either BXO2229 or BXO2230, and all of the reisolated bacteria (100/100 tested) retained the kanamycin resistance marker that is associated with the *gus* fusion. These reisolated bacteria also retained GUS expression *in vitro* under

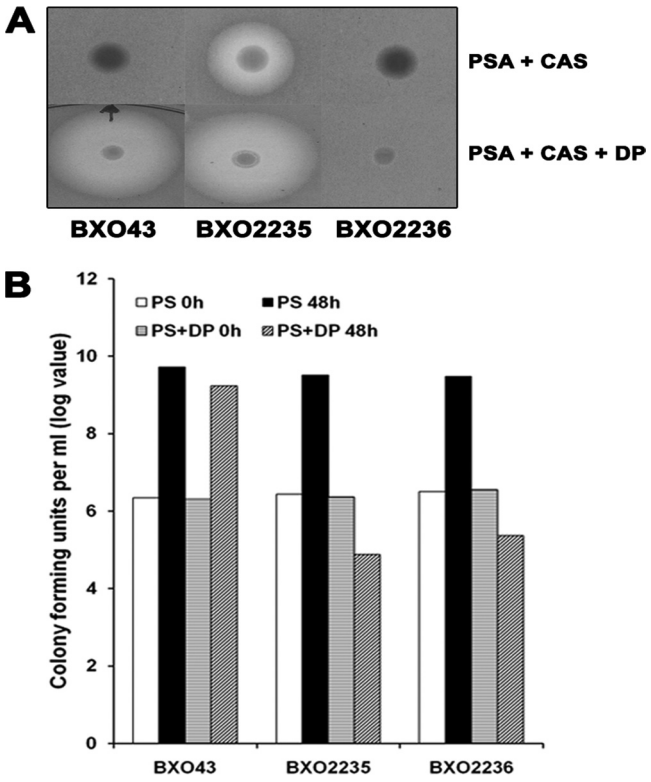

FIG. 8. Siderophore production and growth phenotype of *xsuA* mutants of *X. oryzae* pv. oryzae constructed by integration of suicide plasmid pK18*mob*. (A) Strains depicted are BXO43 (wild-type strain), BXO2235 (*xsuA2*::pK18*mob*; a nonpolar mutation), and BXO2236 (*xsuA3*::pK18*mob*; a polar mutation). *X. oryzae* pv. oryzae strains were grown either on PSA-CAS medium or on PSA-CAS medium supplemented with 100 μM DP. Siderophore production is evident as a halo around the colonies. (B) BXO2235 and BXO2236 are deficient for growth under iron-limiting conditions. Cell numbers were estimated in *X. oryzae* pv. oryzae cultures grown in PS medium and PS–100 μM DP medium at 0 h and after 48 h of growth.

iron-limiting conditions. This indicated that the lack of GUS staining in leaves inoculated with BXO2229 is not due to loss of the *gus* fusion. In addition, the number of CFU/cm^2 of rice leaves infected with these strains also did not differ, indicating that variations in the bacterial density are not the cause of differences in GUS activity (data not shown). Furthermore, GUS expression in bacterial exudates from cut ends of rice leaf pieces infected with BXO2229 and BXO2230 was determined. GUS activity for *feo*::*gusA* and *xssE*::*gusA* fusions in leaf exudates was 64 ± 7.95 nM MU/minute/10^8 CFU and 5.2 ± 0.98 nM MU/minute/10^8 CFU, respectively. This again indicates that the *feo* operon is expressed at a much higher level than the *xss* operon during *in planta* growth.

DISCUSSION

In this study, we have characterized two different *X. oryzae* pv. oryzae iron uptake systems. The *X. oryzae* pv. oryzae *feoABC* genes are homologues of well-characterized ferrous transporters in other bacteria wherein the *feoB* gene encodes the major bacterial ferrous ion transporter. The *xss* operon is homologous to siderophore-biosynthetic genes in other bacteria and is essential for siderophore production by *X. oryzae* pv. oryzae. We have studied the regulation of these *X. oryzae* pv. oryzae iron uptake systems, demonstrated that they are required for growth on low-iron media, and assessed their roles in virulence. This is the first report on the role of specific iron uptake systems in virulence of any member of the important xanthomonad group of plant pathogens.

Iron supplementation of PS medium suppresses siderophore production by the *X. oryzae* pv. oryzae *feoB* mutant (data not shown), indicating that the strain is experiencing iron limitation on PS medium and that it is overproducing siderophore as a compensatory measure. Quantitative GUS assays showed that, in wild-type cells, the expression of the *feo* operon is induced under iron-limiting conditions (i.e., in the presence of DP), but a basal level of expression is retained even under iron-replete conditions (i.e., medium supplemented with $FeSO_4$). A similar expression pattern of the *feo* operon has been reported for *X. fastidiosa*, in which the levels of *feo* transcripts were not affected under iron-replete conditions while an increase in the amounts of *feo* transcripts was detected under iron-limiting conditions (76). Altogether, it seems that the *X. oryzae* pv. oryzae *feoABC* operon is expressed at a basal level even under high-iron conditions and that iron uptake via FeoB may form a constitutive pathway that is utilized by this bacterium under all growth conditions.

Other than the *mhpE* gene, homologs of the remaining six genes in the *xss* operon are present within the *pvs* gene cluster which is involved in biosynthesis of vibrioferrin, an α-hydroxy carboxylate siderophore of *V. parahaemolyticus* (67). Homologs of the *X. oryzae* pv. oryzae *mhpE* gene, named *acsB* and *sbnG*, are present in gene clusters involved in the biosynthesis of the α-hydroxy carboxylate-type of siderophores, achromobactin of *E. chrysanthemi* and staphyloferrin B of *Staphylococcus aureus*, respectively (4, 23). Mutations have not been isolated in the *acsB* and *sbnG* genes. It has been suggested (23) that MhpE-like proteins might maintain a pool of certain carbohydrates that are essential for the formation of siderophore. However, at least in *X. oryzae* pv. oryzae, MhpE is not essential for siderophore production.

Bacterial siderophore biosynthetic gene clusters generally include genes that encode functions involved in export of siderophore and uptake of the ferric-siderophore complex. Most characterized siderophore exporters are members of the MFS family, including proteins such as exporter of enterobactin in *E. coli* (EntS) (25), vibrioferrin in *V. parahaemolyticus* (PvsC) (68), achromobactin in *E. chrysanthemi* (YhcA) (23), alcaligin in *Bordetella* spp. (AlcS) (10), bacillibactin in *Bacillus subtilis* (YmfE) (44), legiobactin in *L. pneumophila* (LbtB) (1), and protochelin in *Azotobacter vinelandii* (CbsX) (49). The observation that XssC is an MFS family protein and its homology to PvsC suggest that *xssC* might be encoding an exporter involved in siderophore secretion. The homology of XsuA protein to PvuA, which acts as a ferric-vibrioferrin receptor in *V. parahaemolyticus* (24), and the observation that *xsuA* mutants are unable to utilize native siderophore suggest that XsuA encodes a siderophore receptor protein.

Several studies have established a role for ferrous iron acquisition via FeoB in the virulence of animal-pathogenic bacteria (12). Our observation that the *feoB* mutant of *X. oryzae* pv. oryzae is severely virulence deficient represents the first

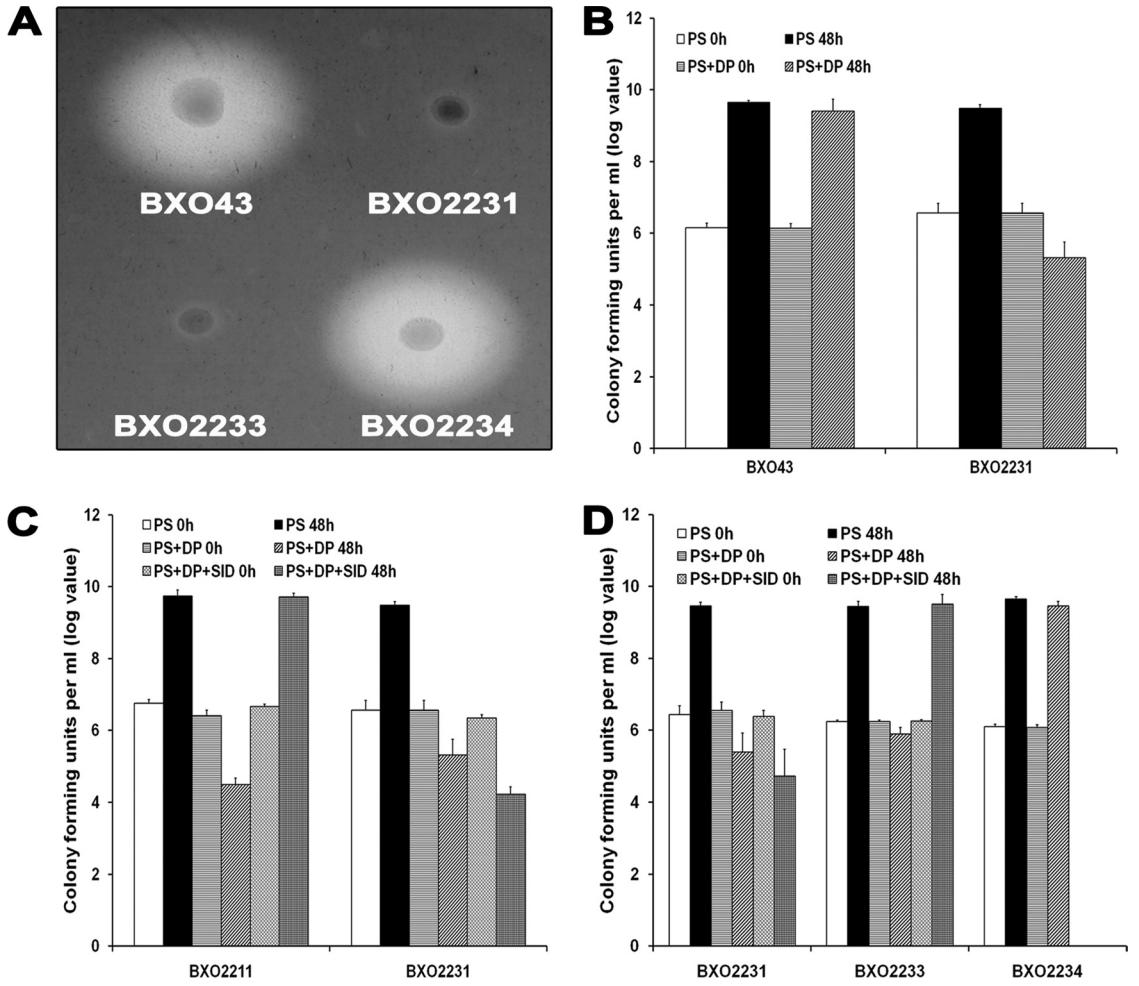

FIG. 9. The phenotype of an *xsuA X. oryzae* pv. *oryzae* mutant is suggestive of deficiency in siderophore uptake. (A) Siderophore production phenotype of an *xsuA* mutant of *X. oryzae* pv. oryzae. Strains depicted are BXO43 (wild-type strain), BXO2231 (*xsuA1*::*gusA*; a polar mutation), BXO2233 (BXO2231/pAP23; this cosmid contains the *xsuA* gene but does not contain any intact *xss* genes), and BXO2234 (BXO2231/pAP15; this cosmid contains the entire *xss* gene cluster including the *xsuA* gene). *X. oryzae* pv. oryzae strains were grown on PSA-CAS medium and 100 μM DP. Siderophore production is evident as a halo around the colonies. (B). An *xsuA* mutant of *X. oryzae* pv. oryzae is deficient for growth under iron-limiting conditions. Cell numbers (log values) were estimated in *X. oryzae* pv. oryzae cultures grown in PS medium and PS–100 μM DP medium at 0 h and after 48 h of growth. (C) An *xsuA* mutant is unable to use exogenously supplied siderophore. Strains are BXO2211 (*xssE1*::pK18*mob*) and BXO2231 (*xsuA1*::*gusA*). (D) Genetic complementation restores the ability of an *X. oryzae* pv. *oryzae xsuA* mutant to utilize exogenously supplied siderophore. Strains are BXO2231 (*xsuA1*::*gusA*), BXO2233 (BXO2231/pAP23), and BXO2234 (BXO2231/pAP15). Cell numbers were estimated in 3 ml of *X. oryzae* pv. oryzae cultures grown in PS medium, PS–100 μM DP medium, and PS–100 μM DP supplemented with SID (cell-free supernatant of a saturated culture of wild-type *X. oryzae* pv. oryzae strain BXO43 grown in iron-deficient medium [PS–100 μM DP]) at 0 h and after 48 h of growth. The results from three independent experiments are expressed as means ± standard deviations.

demonstration of the role of the *feoB* gene in virulence of any plant-pathogenic bacterium. It is likely that this virulence deficiency is due to a defect in iron uptake although the possibility that FeoB is also importing something else other than iron or that it is serving as an exporter cannot be excluded. In contrast, *X. oryzae* pv. oryzae mutants defective for siderophore production/utilization were as virulent as the wild-type strain. Our data indicate that, under iron-deficient conditions in the laboratory, the FeoB protein as well as siderophore are involved in iron uptake as a mutation in either one of these systems affects ability growth on low-iron medium.

It is generally agreed that iron exists as Fe^{3+}-citrate complex in xylem vessels of plants (50). However, recently, speciation analysis of xylem sap of rice demonstrated that iron is present in Fe^{2+} and Fe^{3+} forms and that the concentration of iron in the xylem sap is in the micromolar range (75). Bacterial requirement for iron is generally in the micromolar range (9), suggesting that there is an ample availability of iron for *X. oryzae* pv. oryzae in the rice xylem vessels within which it grows. The lack of expression of the *xss* operon during *in planta* growth is also consistent with the possibility that *X. oryzae* pv. oryzae does not ordinarily experience a limitation for iron during *in planta* growth. In this context, it is worth noting that *R. solanacearum* also does not produce the staphyloferrin B siderophore in tomato xylem sap (which contains >5 μM iron) (5). It is unclear why siderophores are important for virulence in some plant-pathogenic bacteria and are apparently disposable for virulence in others. The levels of available iron within

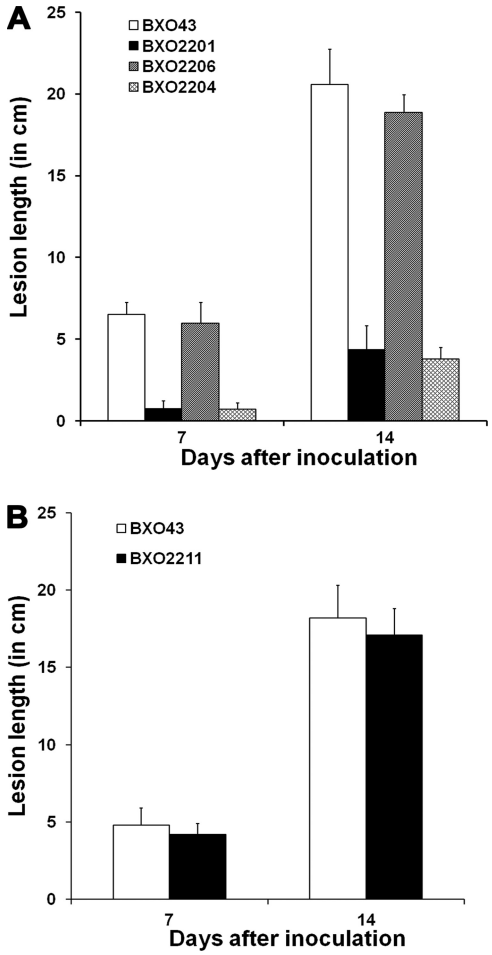

FIG. 10. Virulence phenotype of *X. oryzae* pv. oryzae strains with mutations in genes involved in iron acquisition. Inoculations were performed on leaves of 40-day-old greenhouse-grown plants of susceptible rice cultivar Taichung native-1 (TN-1). Lesion lengths were measured 7 and 14 days after inoculation. Means and standard deviations of 15 replicate measurements are given. Results from one experiment are presented. Similar results were obtained in independent experiments. (A) An *X. oryzae* pv. oryzae *feoB* mutant is severely virulence deficient. Strains are BXO43 (wild-type strain), BXO2201 (*feoB1*::pK18*mob*), BXO2206 (BXO2201/pAP3; complemented strain; pAP3 is pHM1-*feo*B), and BXO2204 (BXO2201/pHM1; vector control). (B) A siderophore-deficient mutant of *X. oryzae* pv. oryzae is virulence proficient. Strains are BXO43 and BXO2211 (*xssE1*::pK18*mob*). The values obtained for BXO2211 were not significantly different ($P < 0.05$, for 7 days and 14 days) from those for BXO43 in a Student's two-tailed *t* test for independent means. Similar results (data not shown) were obtained with BXO2214 (*xssB1*::pK18*mob*), BXO2217 (*xssA1*::pK18*mob*), BXO2220 (*mhpE1*::pK18*mob*), and BXO2231 (*xsuA1*::*gusA*) strains.

plant tissues and the presence of alternate iron uptake systems might be contributing factors in determining the virulence phenotype of siderophore-deficient mutants of plant-pathogenic bacteria. Although siderophore is not required for growth of *X. oryzae* pv. oryzae within the host, it is possible that siderophore may have an important role in other phases of the life cycle of this pathogen wherein it has to survive outside the host.

X. oryzae pv. oryzae mutants for *rpfF* (regulation of pathogenicity factor; a global regulator) are deficient for virulence and growth under low-iron conditions and are siderophore

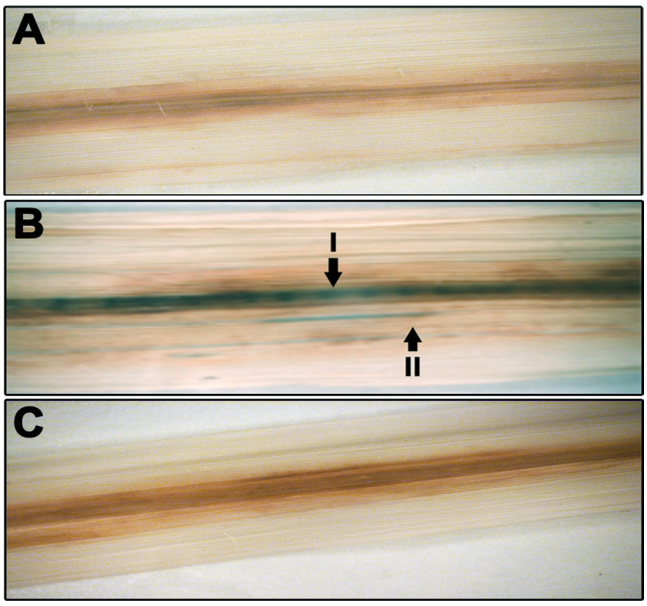

FIG. 11. The *feo*B gene of *X. oryzae* pv. oryzae is expressed during *in planta* growth. Inoculations were performed on leaves of 40-day-old greenhouse-grown plants of susceptible rice cultivar TN-1 with BXO43 (GUS negative) (A) and Gus reporter strains BXO2230 (*feo*::*gusA*) (B) and BXO2229 (*xssE2*::*gusA*) (C). Twelve days after inoculation, the leaves were stained for GUS activity as described in Materials and Methods. Arrows indicate major (I) and minor (II) longitudinal veins. Blue-green staining in the veins in panel indicates GUS expression.

overproducers (15). Exogenous iron supplementation has been shown to promote *in planta* growth of *X. oryzae* pv. oryzae *rpfF* mutants. It appears that the *rpfF* gene promotes virulence of *X. oryzae* pv. oryzae by facilitating iron uptake. A possibility that needs to be tested is that *rpfF* promotes iron acquisition by *X. oryzae* pv. oryzae through control of *feoB* expression. In summary, we have demonstrated that *X. oryzae* pv. oryzae possesses an FeoB-mediated and siderophore-mediated iron uptake system. We have further shown that FeoB protein is required for *X. oryzae* pv. oryzae to grow inside the rice plant. Another possibility is that *X. oryzae* pv. oryzae FeoB can be used as a target for developing new molecules that can be used for application on rice fields against bacterial blight disease and possibly diseases caused by other xanthomonads.

ACKNOWLEDGMENTS

We thank Matthieu Arlat for providing the plasmid pVO155.

A.P. was supported by a Senior Research Fellowship from the Council of Scientific and Industrial Research (CSIR), Government of India. This work was supported, in part, by a grant to R.V.S. from the Department of Biotechnology, Government of India.

REFERENCES

1. **Allard, K. A., V. K. Viswanathan, and N. P. Cianciotto.** 2006. *lbtA* and *lbtB* are required for production of the *Legionella pneumophila* siderophore legiobactin. J. Bacteriol. **188:**1351–1363.
2. **Altschul, S. F., W. Gish, W. Miller, E. W. Myers, and D. J. Lipman.** 1990. Basic local alignment search tool. J. Mol. Biol. **215:**403–410.
3. **Bearden, S. W., J. D. Fetherston, and R. D. Perry.** 1997. Genetic organization of the yersiniabactin biosynthetic region and construction of avirulent mutants in *Yersinia pestis*. Infect. Immun. **65:**1659–1668.
4. **Beasley, F. C., E. D. Vines, J. C. Grigg, Q. Zheng, S. Liu, G. A. Lajoie, M. E. Murphy, and D. E. Heinrichs.** 2009. Characterization of staphyloferrin A biosynthetic and transport mutants in *Staphylococcus aureus*. Mol. Microbiol. **72:**947–963.

5. **Bhatt, G., and T. P. Denny.** 2004. *Ralstonia solanacearum* iron scavenging by the siderophore staphyloferrin B is controlled by PhcA, the global virulence regulator. J. Bacteriol. **186:**7896–7904.
6. **Bhattacharyya, A., S. Stilwagen, N. Ivanova, M. D'Souza, A. Bernal, A. Lykidis, V. Kapatral, I. Anderson, N. Larsen, T. Los, G. Reznik, E. Selkov Jr., T. L. Walunas, H. Feil, W. S. Feil, A. Purcell, J. L. Lassez, T. L. Hawkins, R. Haselkorn, R. Overbeek, P. F. Predki, and N. C. Kyrpides.** 2002. Whole-genome comparative analysis of three phytopathogenic *Xylella fastidiosa* strains. Proc. Natl. Acad. Sci. U. S. A. **99:**12403–12408.
7. **Blanvillain, S., D. Meyer, A. Boulanger, M. Lautier, C. Guynet, N. Denance, J. Vasse, E. Lauber, and M. Arlat.** 2007. Plant carbohydrate scavenging through TonB-dependent receptors: a feature shared by phytopathogenic and aquatic bacteria. PLoS One **2:**e224.
8. **Boyer, E., I. Bergevin, D. Malo, P. Gros, and M. F. Cellier.** 2002. Acquisition of Mn(II) in addition to Fe(II) is required for full virulence of *Salmonella enterica* serovar Typhimurium. Infect. Immun. **70:**6032–6042.
9. **Braun, V., and H. Killmann.** 1999. Bacterial solutions to the iron-supply problem. Trends Biochem. Sci. **24:**104–109.
10. **Brickman, T. J., and S. K. Armstrong.** 2005. *Bordetella* AlcS transporter functions in alcaligin siderophore export and is central to inducer sensing in positive regulation of alcaligin system gene expression. J. Bacteriol. **187:** 3650–3661.
11. **Bull, C. T., S. R. Carnegie, and J. E. Loper.** 1996. Pathogenicity of mutants of *Erwinia carotovora* subsp. *carotovora* deficient in aerobactin and catecholate siderophore production. Phytopathology **86:**260–266.
12. **Cartron, M. L., S. Maddocks, P. Gillingham, C. J. Craven, and S. C. Andrews.** 2006. Feo—transport of ferrous iron into bacteria. Biometals **19:**143–157.
13. **Challis, G. L.** 2005. A widely distributed bacterial pathway for siderophore biosynthesis independent of nonribosomal peptide synthetases. Chembiochem **6:**601–611.
14. **Chan, J. W., and P. H. Goodwin.** 1999. The molecular genetics of virulence of *Xanthomonas campestris*. Biotechnol. Adv. **17:**489–508.
15. **Chatterjee, S., and R. V. Sonti.** 2002. *rpfF* mutants of *Xanthomonas oryzae pv. oryzae* are deficient for virulence and growth under low iron conditions. Mol. Plant Microbe Interact. **15:**463–471.
16. **Cody, Y. S., and D. C. Gross.** 1987. Outer membrane protein mediating iron uptake via pyoverdin$_{pss}$, the fluorescent siderophore produced by *Pseudomonas syringae* pv. syringae. J. Bacteriol. **169:**2207–2214.
17. **Crosa, J. H., and C. T. Walsh.** 2002. Genetics and assembly line enzymology of siderophore biosynthesis in bacteria. Microbiol. Mol. Biol. Rev. **66:**223–249.
18. **Crossman, L. C., V. C. Gould, J. M. Dow, G. S. Vernikos, A. Okazaki, M. Sebaihia, D. Saunders, C. Arrowsmith, T. Carver, N. Peters, E. Adlem, A. Kerhornou, A. Lord, L. Murphy, K. Seeger, R. Squares, S. Rutter, M. A. Quail, M. A. Rajandream, D. Harris, C. Churcher, S. D. Bentley, J. Parkhill, N. R. Thomson, and M. B. Avison.** 2008. The complete genome, comparative and functional analysis of *Stenotrophomonas maltophilia* reveals an organism heavily shielded by drug resistance determinants. Genome Biol. **9:**R74. http://genomebiology.com/2008/9/4/R74.
19. **Dashper, S. G., C. A. Butler, J. P. Lissel, R. A. Paolini, B. Hoffmann, P. D. Veith, N. M. O'Brien-Simpson, S. L. Snelgrove, J. T. Tsiros, and E. C. Reynolds.** 2005. A novel *Porphyromonas gingivalis* FeoB plays a role in manganese accumulation. J. Biol. Chem. **280:**28095–28102.
20. **da Silva, A. C., J. A. Ferro, F. C. Reinach, C. S. Farah, L. R. Furlan, R. B. Quaggio, C. B. Monteiro-Vitorello, M. A. Van Sluys, N. F. Almeida, L. M. Alves, A. M. do Amaral, M. C. Bertolini, L. E. Camargo, G. Camarotte, F. Cannavan, J. Cardozo, F. Chambergo, L. P. Ciapina, R. M. Cicarelli, L. L. Coutinho, J. R. Cursino-Santos, H. El-Dorry, J. B. Faria, A. J. Ferreira, R. C. Ferreira, M. I. Ferro, E. F. Formighieri, M. C. Franco, C. C. Greggio, A. Gruber, A. M. Katsuyama, L. T. Kishi, R. P. Leite, E. G. Lemos, M. V. Lemos, E. C. Locali, M. A. Machado, A. M. Madeira, N. M. Martinez-Rossi, E. C. Martins, J. Meidanis, C. F. Menck, C. Y. Miyaki, D. H. Moon, L. M. Moreira, M. T. Novo, V. K. Okura, M. C. Oliveira, V. R. Oliveira, H. A. Pereira, A. Rossi, J. A. Sena, C. Silva, R. F. De Souza, L. A. Spinola, M. A. Takita, R. E. Tamura, E. C. Teixeira, R. I. Tezza, M. Trindade dos Santos, D. Truffi, S. M. Tsai, F. F. White, J. C. Setubal, and J. P. Kitajima.** 2002. Comparison of the genomes of two *Xanthomonas* pathogens with differing host specificities. Nature **417:**459–463.
21. **DeFeyter, R., C. I. Kado, and D. W. Gabriel.** 1990. Small, stable shuttle vectors for use in *Xanthomonas*. Gene **88:**65–72.
22. **Dellagi, A., M. N. Brisset, J. P. Paulin, and D. Expert.** 1998. Dual role of desferrioxamine in *Erwinia amylovora* pathogenicity. Mol. Plant Microbe Interact. **11:**734–742.
23. **Franza, T., B. Mahe, and D. Expert.** 2005. *Erwinia chrysanthemi* requires a second iron transport route dependent of the siderophore achromobactin for extracellular growth and plant infection. Mol. Microbiol. **55:**261–275.
24. **Funahashi, T., K. Moriya, S. Uemura, S. Miyoshi, S. Shinoda, S. Narimatsu, and S. Yamamoto.** 2002. Identification and characterization of *pvuA*, a gene encoding the ferric vibrioferrin receptor protein in *Vibrio parahaemolyticus*. J. Bacteriol. **184:**936–946.
25. **Furrer, J. L., D. N. Sanders, I. G. Hook-Barnard, and M. A. McIntosh.** 2002. Export of the siderophore enterobactin in *Escherichia coli*: involvement of a 43 kDa membrane exporter. Mol. Microbiol. **44:**1225–1234.
26. **Gardy, J. L., M. R. Laird, F. Chen, S. Rey, C. J. Walsh, M. Ester, and F. S. Brinkman.** 2005. PSORTb v. 2.0: expanded prediction of bacterial protein subcellular localization and insights gained from comparative proteome analysis. Bioinformatics **21:**617–623.
27. **He, Y. W., A. Y. Ng, M. Xu, K. Lin, L. H. Wang, Y. H. Dong, and L. H. Zhang.** 2007. *Xanthomonas campestris* cell-cell communication involves a putative nucleotide receptor protein Clp and a hierarchical signalling network. Mol. Microbiol. **64:**281–292.
28. **Innes, R. W., M. A. Hirose, and P. L. Kuempel.** 1988. Induction of nitrogen-fixing nodules on clover requires only 32 kilobase pairs of DNA from the *Rhizobium trifolii* symbiosis plasmid. J. Bacteriol. **170:**3793–3802.
29. **Jefferson, R. A., T. A. Kavanagh, and M. W. Bevan.** 1987. GUS fusions: beta-glucuronidase as a sensitive and versatile gene fusion marker in higher plants. EMBO J. **6:**3901–3907.
30. **Jones, A. M., S. E. Lindow, and M. C. Wildermuth.** 2007. Salicylic acid, yersiniabactin, and pyoverdin production by the model phytopathogen *Pseudomonas syringae* pv. tomato DC3000: synthesis, regulation, and impact on tomato and *Arabidopsis* host plants. J. Bacteriol. **189:**6773–6786.
31. **Kammler, M., C. Schon, and K. Hantke.** 1993. Characterization of the ferrous iron uptake system of *Escherichia coli*. J. Bacteriol. **175:**6212–6219.
32. **Kauffman, H. E., A. P. K. Reddy, S. P. Y. Hsieh, and S. D. Merca.** 1973. An improved technique for evaluation of resistance of rice varieties to *Xanthomonas oryzae*. Plant Dis. Rep. **57:**537–541.
33. **Krewulak, K. D., and H. J. Vogel.** 2008. Structural biology of bacterial iron uptake. Biochim. Biophys. Acta **1778:**1781–1804.
34. **Lawlor, M. S., C. O'connor, and V. L. Miller.** 2007. Yersiniabactin is a virulence factor for *Klebsiella pneumoniae* during pulmonary infection. Infect. Immun. **75:**1463–1472.
35. **Leach, J. E., F. F. White, M. L. Rhoads, and H. Leung.** 1990. A repetitive DNA sequence differentiates *Xanthomonas campestris* pv. oryzae from other pathovars of *X. campestris*. Mol. Plant Microbe Interact. **3:**238–246.
36. **Lee, B. M., Y. J. Park, D. S. Park, H. W. Kang, J. G. Kim, E. S. Song, I. C. Park, U. H. Yoon, J. H. Hahn, B. S. Koo, G. B. Lee, H. Kim, H. S. Park, K. O. Yoon, J. H. Kim, C. H. Jung, N. H. Koh, J. S. Seo, and S. J. Go.** 2005. The genome sequence of *Xanthomonas oryzae* pathovar *oryzae* KACC10331, the bacterial blight pathogen of rice. Nucleic Acids Res. **33:**577–586.
37. **Lee, S. J., J. H. Ko, H. Y. Kang, and Y. Lee.** 2006. Coupled expression of MhpE aldolase and MhpF dehydrogenase in *Escherichia coli*. Biochem. Biophys. Res. Commun. **346:**1009–1015.
38. **Leong, S. A., and J. B. Neilands.** 1981. Relationship of siderophore-mediated iron assimilation to virulence in crown gall disease. J. Bacteriol. **147:**482–491.
39. **Loprasert, S., R. Sallabhan, S. Atichartpongkul, and S. Mongkolsuk.** 1999. Characterization of a ferric uptake regulator (*fur*) gene from *Xanthomonas campestris* pv. phaseoli with unusual primary structure, genome organization, and expression patterns. Gene. **239:**251–258.
40. **Marlovits, T. C., W. Haase, C. Herrmann, S. G. Aller, and V. M. Unger.** 2002. The membrane protein FeoB contains an intramolecular G protein essential for Fe(II) uptake in bacteria. Proc. Natl. Acad. Sci. U. S. A. **99:**16243–16248.
41. **Martinez, J. L., M. Herrero, and V. de Lorenzo.** 1994. The organization of intercistronic regions of the aerobactin operon of pColV-K30 may account for the differential expression of the *iucABCD iutA* genes. J. Mol. Biol. **238:**288–293.
42. **Meyer, J. M., A. Neely, A. Stintzi, C. Georges, and I. A. Holder.** 1996. Pyoverdin is essential for virulence of *Pseudomonas aeruginosa*. Infect. Immun. **64:**518–523.
43. **Miethke, M., and M. A. Marahiel.** 2007. Siderophore-based iron acquisition and pathogen control. Microbiol. Mol. Biol. Rev. **71:**413–451.
44. **Miethke, M., S. Schmidt, and M. A. Marahiel.** 2008. The major facilitator superfamily-type transporter YmfE and the multidrug-efflux activator Mta mediate bacillibactin secretion in *Bacillus subtilis*. J. Bacteriol. **190:**5143–5152.
45. **Naikare, H., K. Palyada, R. Panciera, D. Marlow, and A. Stintzi.** 2006. Major role for FeoB in *Campylobacter jejuni* ferrous iron acquisition, gut colonization, and intracellular survival. Infect. Immun. **74:**5433–5444.
46. **Neilands, J. B.** 1995. Siderophores: structure and function of microbial iron transport compounds. J. Biol. Chem. **270:**26723–26726.
47. **Nino-Liu, D. O., P. C. Ronald, and A. J. Bogdanove.** 2006. *Xanthomonas oryzae* pathovars: model pathogens of a model crop. Mol. Plant Pathol. **7:**303–324.
48. **Oke, V., and S. R. Long.** 1999. Bacterial genes induced within the nodule during the *Rhizobium*-legume symbiosis. Mol. Microbiol. **32:**837–849.
49. **Page, W. J., E. Kwon, A. S. Cornish, and A. E. Tindale.** 2003. The *csbX* gene of *Azotobacter vinelandii* encodes an MFS efflux pump required for catecholate siderophore export. FEMS Microbiol. Lett. **228:**211–216.
50. **Palmer, C. M., and M. L. Guerinot.** 2009. Facing the challenges of Cu, Fe and Zn homeostasis in plants. Nat. Chem. Biol. **5:**333–340.
51. **Panina, E. M., A. A. Mironov, and M. S. Gelfand.** 2001. Comparative analysis of FUR regulons in gamma-proteobacteria. Nucleic Acids Res. **29:**5195–5206.

52. **Payne, S. M.** 1994. Detection, isolation, and characterization of siderophores. Methods Enzymol. **235:**329–344.
53. **Putman, M., H. W. van Veen, and W. N. Konings.** 2000. Molecular properties of bacterial multidrug transporters. Microbiol. Mol. Biol. Rev. **64:**672–693.
54. **Rajagopal, L., S. Dharmapuri, A. T. Sayeepriyadarshini, and R. V. Sonti.** 1999. A genomic library of *Xanthomonas oryzae* pv. oryzae in the broad host range mobilizing *Escherichia coli* strain S17-1. Int. Rice Res. Notes **24:**20–21.
55. **Ray, S. K., R. Rajeshwari, and R. V. Sonti.** 2000. Mutants of *Xanthomonas oryzae* pv. oryzae deficient in general secretory pathway are virulence deficient and unable to secrete xylanase. Mol. Plant Microbe Interact. **13:**394–401.
56. **Regha, K., A. K. Satapathy, and M. K. Ray.** 2005. RecD plays an essential function during growth at low temperature in the Antarctic bacterium *Pseudomonas syringae* Lz4W. Genetics **170:**1473–1484.
57. **Robey, M., and N. P. Cianciotto.** 2002. *Legionella pneumophila feoAB* promotes ferrous iron uptake and intracellular infection. Infect. Immun. **70:** 5659–5669.
58. **Rondon, M. R., K. S. Ballering, and M. G. Thomas.** 2004. Identification and analysis of a siderophore biosynthetic gene cluster from *Agrobacterium tumefaciens* C58. Microbiology **150:**3857–3866.
59. **Rose, T. M., E. R. Schultz, J. G. Henikoff, S. Pietrokovski, C. M. McCallum, and S. Henikoff.** 1998. Consensus-degenerate hybrid oligonucleotide primers for amplification of distantly related sequences. Nucleic Acids Res. **26:**1628–1635.
60. **Ryan, R. P., S. Monchy, M. Cardinale, S. Taghavi, L. Crossman, M. B. Avison, G. Berg, D. van der Lelie, and J. M. Dow.** 2009. The versatility and adaptation of bacteria from the genus *Stenotrophomonas*. Nat. Rev. Microbiol. **7:**514–525.
61. **Sambrook, J., E. F. Fritsch, and T. Maniatis.** 1989. Molecular cloning: a laboratory manual, 2nd ed. Cold Spring Harbor Laboratory Press, Cold Spring Harbor, NY.
62. **Schafer, A., A. Tauch, W. Jager, J. Kalinowski, G. Thierbach, and A. Puhler.** 1994. Small mobilizable multi-purpose cloning vectors derived from the *Escherichia coli* plasmids pK18 and pK19: selection of defined deletions in the chromosome of *Corynebacterium glutamicum*. Gene **145:**69–73.
63. **Schwyn, B., and J. B. Neilands.** 1987. Universal chemical assay for the detection and determination of siderophores. Anal. Biochem. **160:**47–56.
64. **Simon, R., U. Priefer, and A. Puhler.** 1983. A broad host range mobilization system for *in vivo* genetic engineering: transposon mutagenesis in gram negative bacteria. Nat. Biotechnol. **1:**784–791.
65. **Stojiljkovic, I., M. Cobeljic, and K. Hantke.** 1993. *Escherichia coli* K-12 ferrous iron uptake mutants are impaired in their ability to colonize the mouse intestine. FEMS Microbiol. Lett. **108:**111–115.
66. **Subramoni, S., and R. V. Sonti.** 2005. Growth deficiency of a *Xanthomonas oryzae* pv. oryzae *fur* mutant in rice leaves is rescued by ascorbic acid supplementation. Mol. Plant Microbe Interact. **18:**644–651.
67. **Tanabe, T., T. Funahashi, H. Nakao, S. Miyoshi, S. Shinoda, and S. Yamamoto.** 2003. Identification and characterization of genes required for biosynthesis and transport of the siderophore vibrioferrin in *Vibrio parahaemolyticus*. J. Bacteriol. **185:**6938–6949.
68. **Tanabe, T., H. Nakao, T. Kuroda, T. Tsuchiya, and S. Yamamoto.** 2006. Involvement of the *Vibrio parahaemolyticus pvsC* gene in export of the siderophore vibrioferrin. Microbiol. Immunol. **50:**871–876.
69. **Thompson, J. D., D. G. Higgins, and T. J. Gibson.** 1994. CLUSTAL W: improving the sensitivity of progressive multiple sequence alignment through sequence weighting, position-specific gap penalties and weight matrix choice. Nucleic Acids Res. **22:**4673–4680.
70. **Touati, D.** 2000. Iron and oxidative stress in bacteria. Arch. Biochem. Biophys. **373:**1–6.
71. **Velayudhan, J., N. J. Hughes, A. A. McColm, J. Bagshaw, C. L. Clayton, S. C. Andrews, and D. J. Kelly.** 2000. Iron acquisition and virulence in *Helicobacter pylori*: a major role for FeoB, a high-affinity ferrous iron transporter. Mol. Microbiol. **37:**274–286.
72. **Wiggerich, H. G., B. Klauke, R. Koplin, U. B. Priefer, and A. Puhler.** 1997. Unusual structure of the *tonB-exb* DNA region of *Xanthomonas campestris* pv. campestris: *tonB*, *exbB*, and *exbD1* are essential for ferric iron uptake, but *exbD2* is not. J. Bacteriol. **179:**7103–7110.
73. **Wiggerich, H. G., and A. Puhler.** 2000. The *exbD2* gene as well as the iron-uptake genes *tonB*, *exbB* and *exbD1* of *Xanthomonas campestris* pv. *campestris* are essential for the induction of a hypersensitive response on pepper (*Capsicum annuum*). Microbiology **146:**1053–1060.
74. **Windgassen, M., A. Urban, and K. E. Jaeger.** 2000. Rapid gene inactivation in *Pseudomonas aeruginosa*. FEMS Microbiol. Lett. **193:**201–205.
75. **Yokosho, K., N. Yamaji, D. Ueno, N. Mitani, and J. F. Ma.** 2009. OsFRDL1 is a citrate transporter required for efficient translocation of iron in rice. Plant Physiol. **149:**297–305.
76. **Zaini, P. A., A. C. Fogaca, F. G. Lupo, H. I. Nakaya, R. Z. Vencio, and A. M. da Silva.** 2008. The iron stimulon of *Xylella fastidiosa* includes genes for type IV pilus and colicin V-like bacteriocins. J. Bacteriol. **190:**2368–2378.